Palaeontologia Electronica
palaeo-electronica.org

First report of rodents from the Miocene Siwalik locality of Dunera, Pathankot District, Punjab, India

Ramesh Kumar Sehgal, Abhishek Pratap Singh, Ningthoujam Premjit Singh, Christopher C. Gilbert, Biren A. Patel, and Rajeev Patnaik

ABSTRACT

Although there have been a few reports of macromammals from the Siwalik site of Dunera, no micromammals have yet been described. Recently, a diverse micromammal fossil assemblage represented by isolated teeth has been recovered from Dunera. The specimens are identified as a murine similar to *Progonomys hussaini (Progonomys* cf. *hussaini),* the ctenodactylid *Sayimys sivalensis*, the cricetid *Democricetodon fejfari*, and a sciurid, cf. *Tamias urialis.* These rodents are documented for the first time from this region of the Indian Siwaliks. Based on the biostratigraphic ranges of these rodents from well-dated localities in the Siwaliks of Pakistan along with previously collected magnetostratigraphic data, Dunera locality best correlates to between ~11-10 Ma (early Late Miocene), approximately equivalent to the lower half of the Nagri Formation. Previous magneto-stratigraphic data suggests that an age closer to ~11 Ma is more likely, perhaps sampling a temporal gap in the known Siwaliks micromammal record and extending the age ranges of *P. hussaini* and *T. urialis* by a few hundred thousand years.

Ramesh Kumar Sehgal. Wadia Institute of Himalayan Geology, Dehradun-248001; Academy of Scientific and Innovative Research, Ghaziabad, Uttar Pradesh-201002, India. rksehgal@wihg.res.in
Abhishek Pratap Singh. Wadia Institute of Himalayan Geology, Dehradun-248001; Academy of Scientific and Innovative Research, Ghaziabad, Uttar Pradesh-201002, India. abhishekpratap@wihg.res.in
Ningthoujam Premjit Singh. Wadia Institute of Himalayan Geology, Dehradun-248001; Academy of Scientific and Innovative Research, Ghaziabad, Uttar Pradesh-201002, India. Corresponding author. ningthoujampremjit11@gmail.com
Christopher C. Gilbert. Department of Anthropology, Hunter College of the City University of New York, 695 Park Avenue, New York, NY 10065, USA; PhD Program in Anthropology, Graduate Center of the City University of New York, 365 Fifth Avenue, NY 10016, USA; New York Consortium in Evolutionary Primatology, New York, NY, USA; Division of Paleontology, American Museum of Natural History, Central Park West at 79th Street, New York, NY, 10024, USA. cgilbert@hunter.cuny.edu

Final citation: Sehgal, Ramesh Kumar, Singh, Abhishek Pratap, Singh, Ningthoujam Premjit, Gilbert, Christopher C., Patel, Biren A., and Patnaik, Rajeev. 2023. First report of rodents from the Miocene Siwalik locality of Dunera, Pathankot District, Punjab, India. Palaeontologia Electronica, 26(3):a49.
https://doi.org/10.26879/1308
palaeo-electronica.org/content/2023/4011-rodents-from-dunera-india

Biren A. Patel. Department of Integrative Anatomical Sciences, Keck School of Medicine, University of Southern California, Los Angeles, CA 90033, USA; Human and Evolutionary Biology Section, Department of Biological Sciences, University of Southern California, Los Angeles, CA 90089, USA. birenpat@usc.edu
Rajeev Patnaik. Department of Geology, Panjab University, Chandigarh-160014, India. rajeevpatnaik@gmail.com

Keywords: Dunera (Punjab, India); Micromammals; Middle Siwalik; Miocene; Nagri Formation

Submission: 25 May 2023. Acceptance: 6 November 2023.

INTRODUCTION

The Siwalik Group, which stretches for almost 2500 km along the Himalayan foothills, represents the Neogene and Quaternary river deposition of the Himalayan Foreland Basin. The Siwaliks record an extensive sample of fossil vertebrates, including various mammalian species, and provide crucial information regarding the historical biodiversity and ecology of many extant and extinct groups. As a result of multidisciplinary geological investigations (magnetic polarity stratigraphy, tephrochronology, and mammalian biostratigraphy) on the Siwalik Group deposits in Pakistan over the course of the last four decades (e.g., Barry et al., 1982, 1985, 2002, 2013; Barry and Flynn 1990; Flynn et al., 2013), a Siwalik chronostratigraphy with a high degree of precision and resolution has been established. In India, the Middle and Upper Siwalik deposits spanning much of the Late Miocene and Plio-Pleistocene have been well dated by magnetostratigraphic study and correlation to the geomagnetic polarity time scale (Yokoyama, 1981; Azzaroli and Napolene, 1982; Johnson et al., 1983; Tandon et al., 1984; Ranga Rao et al., 1988, 1995; Sangode et al., 1996; Kumaravel et al., 2005; Pillans et al., 2005; Kotlia et al., 2008; Chirouze et al., 2012), but such studies are still lacking for the Indian Lower Siwaliks. In the absence of geochronologically dated sections at these localities, biostratigraphy is used to infer the age of fossil-yielding rock units. The Lower Siwaliks in India are best-known near the town of Ramnagar (Udhampur District, Jammu and Kashmir). For more than 100 years, numerous studies by various workers in the Ramnagar area have considered the fossil-bearing deposits as roughly equivalent in age to the Chinji Formation (~14.0-11.4 Ma) based on the recovered mammalian assemblage (Brown et al., 1924; Pilgrim, 1927; Colbert, 1935; Gregory et al., 1938; Thomas and Verma, 1979; Vasishat et al., 1978, 1979; Gaur and Chopra, 1983; Chopra, 1983; Vasishat et al., 1985; Sehgal, 1998; Nanda and Sehgal, 1993; Verma et al., 2002; Basu, 2004; Parmar and Prasad, 2006, 2012; Sehgal and Patnaik, 2012; Parmar, 2013; Parmar and Jigmet, 2014; Parmar et al., 2015, 2018, 2023; Gilbert et al., 2017, 2019, 2020; Singh et al., 2018; Sehgal et al., 2022).

Here, we report fossils from a locality exposed close to the town of Dunera (Pathankot District, Punjab, India) that has previously been suggested to represent either the Lower or Middle Siwaliks. Although the Dunera area is known for a few previously described macromammals such as tragulids (*Dorcatherium* sp.), giraffids (*Giraffokeryx* sp.), and bovids (gen. et sp. indet.) (Vasishat et al., 1983), no micromammals have yet been reported. Consequently, due to the absence of chronologically informative fauna, the precise age of the Dunera deposits beyond a general correlation to the Chinji and/or Nagri formations (Vasishat et al., 1983; Sinha et al., 2005) has remained uncertain. Recently, we recovered chronologically informative micromammals from Dunera belonging to four rodent families: Muridae, Ctenodactylidae, Cricetidae, and Sciuridae. These specimens represent the first rodents documented from this region and are described here. Additionally, we provide a preliminary taxonomic assessment of these fossils and use this information to discuss the age of the fossiliferous locality exposed at Dunera based on rodent biostratigraphy that has already been established throughout the Lower and Middle Siwaliks of the Potwar Plateau (Flynn et al., 1995, 2023). Based on our assessment, it appears that Dunera locality correlates with the lower half of the Nagri Formation in the Middle Siwaliks and thus samples the early Late Miocene rather than the late Middle Miocene.

GEOLOGICAL SETTING

A complete sequence of Siwalik rocks is exposed along the Katilu Khad section in Dunera. The section is divided into the Lower, Middle, and Upper Siwalik Sub-groups based on lithological

variation (Rangaraj, 1978; Tandon and Rangaraj, 1979). Lithologically, it comprises sandstone-mudstone in the lower part, sandstone-mudstone-conglomerate in the middle, and thickly bedded conglomerate in the upper parts (Sinha et al., 2005, 2007). Sinha et al. (2005) carried out a magnetostratigraphic study of a 2.7 km thick Miocene-Pliocene Siwalik succession of Katilu Khad section and assigned an age for the sequence between 12.77 and 4.58 Ma. They considered the base of the section to begin at ~12.8 Ma, which correlates to the Chinji type area deposits in Pakistan and the Ramnagar deposits in Jammu and Kashmir, India. The present study locality is exposed about 3 km to the north of Katilu Khad section (Figure 1) and lies between the aforementioned Middle Miocene fossil locality Ramnagar to the west and the Late Miocene locality Nurpur to the south. Furthermore, Dunera is approximately 330 km east of the Chinji type area on the Potwar Plateau of Pakistan. Previously, Vasishat et al. (1983) reported a few macromammals from Dunera and considered it to be Chinji or Nagri equivalent in age. Sinha et al. (2005) presented magnetostratigraphic evidence that the fauna collected by Vasishat et al. (1983) likely correlates to Chron 5n, which is currently estimated by Ogg (2020) to be ~11.056 Ma at the base. The rock units in this area are characterized by the alternation of sandstone and clay. Between these two rock units, a thin layer of intraformational conglomerate (pseudoconglomerate) is present, and this rock has produced both macro- and microvertebrate fossils. The sandstones lying below are fine to medium grained, moderately compact, and range in color from dirty greyish to brownish.

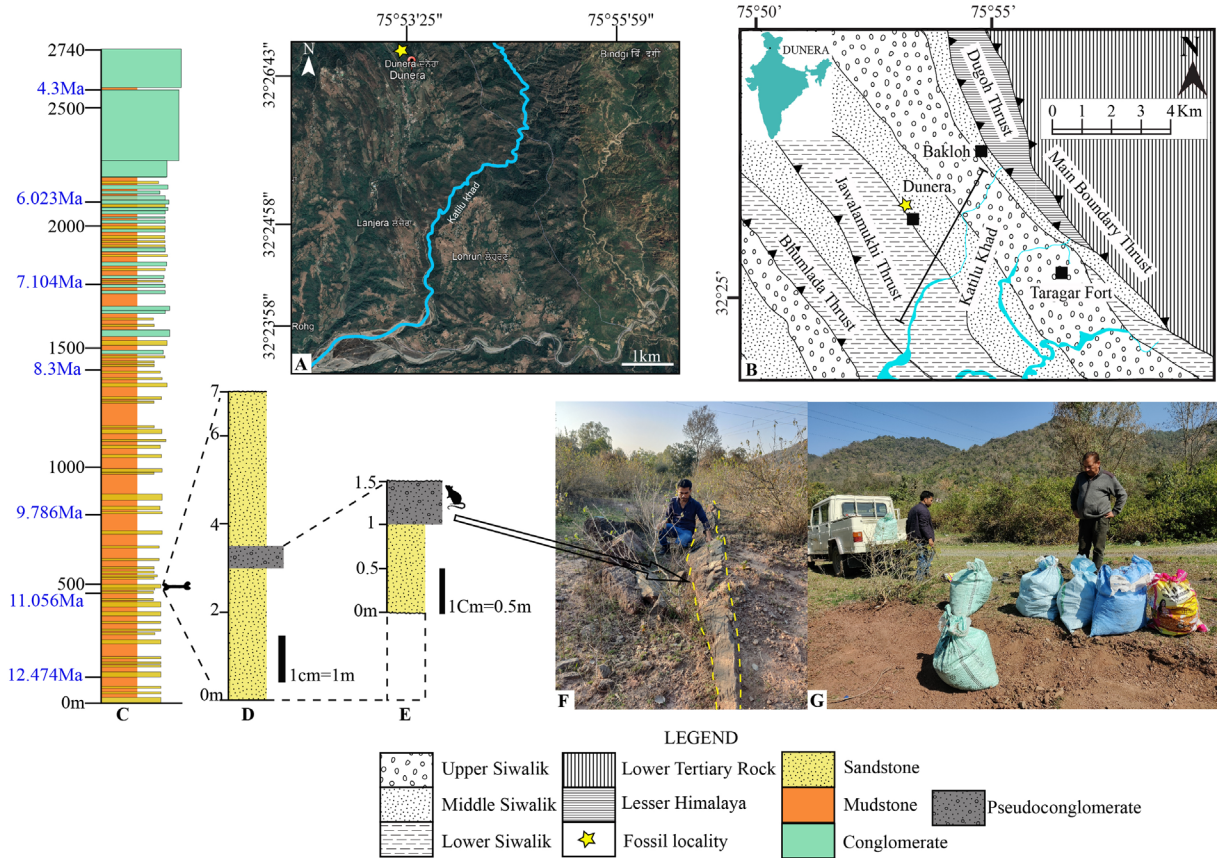

FIGURE 1. A) Google map showing the fossil site (marked by star in yellow color) and Katilu-Khad (marked in blue colour) at Dunera, Punjab, India; B) General geological map of the study area showing fossil locality and Katilu- Khad section (modified after Raiverman, 2002); C) Magnetostratigraphic dated section in Katilu-Khad of Dunera (after Sinha et al., 2005) and revised ages from the most updated version of GPTS (Ogg 2020); D) Stratigraphic section of the bone bed in lower part of Katilu-Khad; E) Stratigraphic section of the present study fossil site at Dunera; F, G) Field photographs of the locality (arrow represents the fossiliferous bed).

MATERIALS AND METHODS

In 2021-2023 field seasons, bulk samples were collected from a locality (32°26'54.3"N 75°53'11.7"E) exposed near Dunera town with an objective to recover micromammals. About 500 kg of sediments were macerated in the Biostratigraphy Laboratory at the Wadia Institute of Himalayan Geology (WIHG; Dehradun, India). At first, the sediments were soaked with water in plastic tubs and kept for a few days. The loose material was wet sieved using mesh sizes of 20 (841 microns), 40 (400 microns), and 60 (250 microns) American Standard Test Sieve Series (ASTM), and the sediment retained in the sieves was sun-dried. Fossils were identified and separated under a binocular microscope using a fine brush. The specimens mentioned here are housed at the WIHG with the catalogue extension WIMF/A (Wadia Institute Micro Fossil Series A).

High-resolution micro-CT (µCT) scanning was utilised to create three-dimensional (3D) surface rendering in order to facilitate the study of these micromammal teeth. Obtaining µCT scans also facilitated digitally removing matrix on the occlusal surface of some specimens (e.g., WIMF/A 4745). All scanning was done at the Molecular Imaging Center of the Keck School of Medicine of the University of Southern California (Los Angeles, CA, USA) using a Nikon XT H 225 scanner with the following parameters: beam energy = 60kV; beam current = 70µA; time frame averaging = 2; projections = 1441; isometric voxel dimensions = 0.00539-0.0068 mm. When possible, each fossil tooth was scanned separately within a plastic sample container (e.g., centrifuge tube or gel cap). If multiple specimens had to be grouped for scanning, it was made certain that no specimens occupied the same 3D field of view. Amira v. 2022.1 software (Thermo Fisher Scientific, Inc., Waltham, MA, USA) was used to produce 3D surface renderings of each specimen from 16-bit DICOM images.

Standard dental measurements of maximum mesiodistal length (MD) and buccolingual breadth (BL) of each tooth were recorded from 3D surface renderings. Comparative measurements on relevant micromammal taxa were obtained from the literature. To examine intraspecific and interspecific variation in dental shape and size data across known micromammal species, bivariate plots were created using the square root of tooth area (MD x BL) and tooth shape (BL/MD), thereby expressing these variables in the same linear units. For samples from the literature with only summary statistics, variation was estimated by plotting the mean, minimum, and maximum values.

SYSTEMATIC PALEONTOLOGY

Family SCIURIDAE Fischer de Waldheim, 1817
Subfamily XERINAE Osborn, 1910
Genus *TAMIAS* Illiger, 1811

Remarks. *Tamias, Eutamias,* and *Neotamias* are here considered subgenera of the genus *Tamias* (cf. Nowak, 1999; Wilson and Reeder, 2005).
Type species. *Tamias (Eutamias) urialis* (Munthe, 1980)

cf. *Tamias urialis* (Munthe, 1980)
Figure 2

Holotype. H-GSP 2013, left mandible fragment with m1-m2.
Type locality. H-GSP locality 18, upper Chinji Formation, Miocene.
Referred materials. WIMF/A 4743 right M1/2 (Figure 2A); WIMF/A 4749 left m1/2 (Figure 2B).
Occurrence. Dunera locality, Punjab, India (study area); Middle Miocene of Dehari locality, Ramnagar, India; Middle Miocene to Late Miocene of Potwar Plateau, Pakistan; early Late Miocene Tapar locality, Kutch, India.
Descriptions. WIMF/A 4743 (Figure 2A) is an upper M1 or M2 with a U-shaped occlusal outline, tapering slightly from the buccal to the lingual side of the tooth. It is buccolingually broad compared to mesiodistal length (Table 1). A paracone, metacone, and protocone are present, and these three cusps are similar in size and prominence. A hypocone appears to be absent, or otherwise indistinct in the distolingual portion of the tooth. A paraconule is absent, but a very small metaconule is present on the metaloph. The protoloph and metaloph are relatively well-defined, resulting in a prominent 'V'-shape in the center of the occlusal surface. The protoloph is complete and relatively uniform in shape, while the metaloph becomes pinched as it approaches the protocone (i.e., between the metaconule and protocone). The anterior cingulum is well-developed, and a parastyle appears to be present in the mesiobuccal corner of the tooth. A small ridge or cuspule, perhaps interpretable as a small mesostyle, is present on the buccal margin of the tooth between the paracone and metacone.

WIMF/A 4749 (Figure 2B), a left m1/2, is rounded on its distal end and slightly wider than long (Table 1). The three visible cusps, the protoconid, metaconid, and hypoconid are distinct, whereas the paraconid, entoconid, and hypoconu-

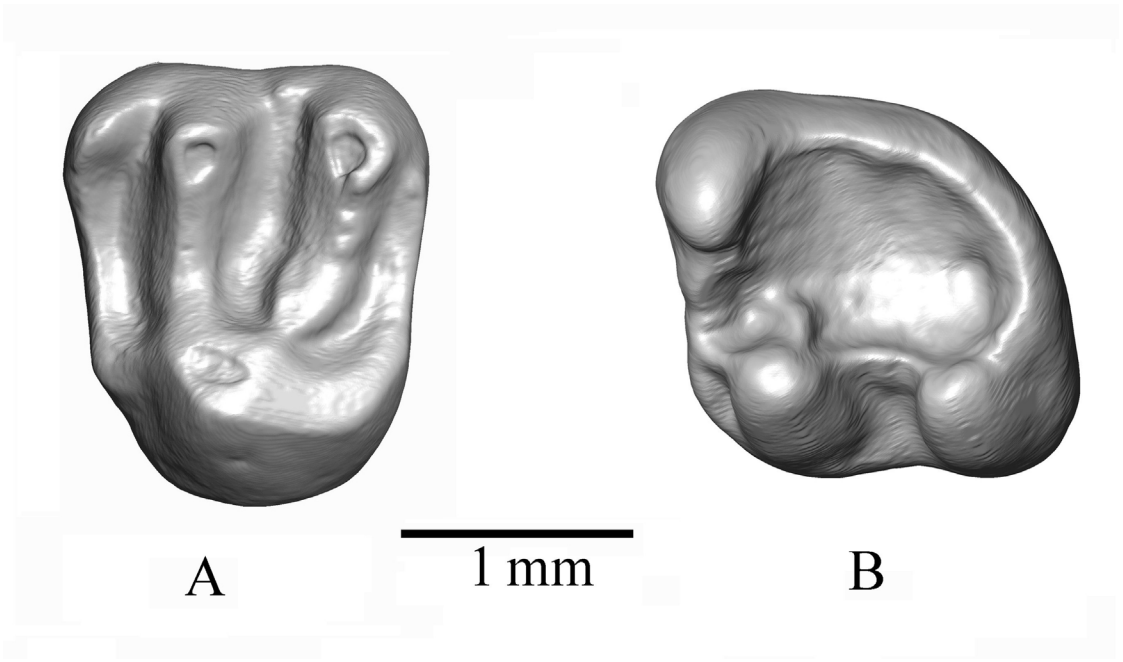

FIGURE 2. 3D surface models of cf. *Tamias urialis* in occlusal views. A) WIMF/A 4743 right M1/2 (mirror-imaged); B) WIMF/A 4749 left m1/2. Note: Mesial towards the left and distal towards the right in all panels.

lid are indistinct or absent. The protoconid is the tallest of the three cusps. The hypoconid is slightly shorter and connected to the protoconid by a mesiodistally oriented cristid obliqua (=ectolophid) running between the bases of these two cusps. A very short mesial or anterior cingulum is present in the mesiobuccal corner of the tooth, forming a small mesiobuccal fovea (i.e., the anterosinusid) between the protoconid and the paralophid. A short protolophid (= metalophid) is very low and incomplete, running from the base of the protoconid turning mesially towards the anterior border of the tooth near the midline. A mesoconid and mesostylid are absent. The lingual side of the tooth is bordered by a ridge that continues around the distal end to connect with the posterolophid, forming a broad and open talonid basin. The tooth has four roots.

Comparison and Remarks. Munthe (1980) described the first fossil sciurid *Eutamias urialis* from the Middle Miocene Siwalik deposits of Daud Khel area of Pakistan. Wessels et al. (1982) collected additional fossil sciurid remains from the Chinji Formation (Middle Miocene) exposed in Banda Daud Shah and identified them as *Tamias urialis* (Munthe, 1980), Sciurinae gen. et sp. indet. and Marmotini gen. et sp. indet. Cheema et al. (1983) recovered sciurid remains cf. *Eutamias urialis* from Siwalik deposits near Jalalpur in Pakistan, and then Cheema et al. (2000) further classified them as *Eutamias urialis* (gracile specimens) and Sciurinae gen. et sp. indet. (robust specimens). Flynn (2003) recognized additional sciurids, *Callosciurus* sp. from the Middle Miocene (14 Ma), *Ratufa sylva* from the Late Miocene (10.5 Ma) and cf. *Ratufa* sp. from the Early Miocene (17 Ma), Potwar Plateau, Pakistan. Where overlapping dental positions exist, the cf. *Ratufa* sp. upper molars from the Early Miocene of Pakistan are easily distinguished from the present M1/2 by their extensive enamel crenulation, the presence of a paraconule, a large metaconule, and a distinct mesostyle. In the Indian Siwaliks, Parmar et al. (2018) and Bhandari et al. (2021) reported *Tamias urialis* from the Middle Miocene Chinji Formation of Ramnagar and the Late Miocene of Tapar locality in Kutch, respectively. Most recently, Patnaik et al. (2022) described a new species of sciurid, *Tamias gilaharee*, from Tapar. The M1/2 of *Tamias gilaharee* is distinguished from WIMF/A 4731 and *T. urialis* by the combination of larger upper molars, a metaloph with a very large metaconule, a thick protoloph with a distinct protoconule, a constricted lingual metaloph, and a more distinct hypocone. As per Munthe (1980) and Wessels et al. (1982), the upper molars of *Tamias urialis* are more typically characterized by having high, thin protolophs, metalophs, posterolophs, a low lying anteroloph, a

TABLE 1. Comparative dental measurements (mm) of Dunera sciurid and other *Tamias* specimens.

Taxon	Locality	Elements (n=sample size)	Mean length (range) in mm	Mean width (range) in mm	Mean width/ length	Square root of width* length	Age	Reference
Tamias cf. *eviensis*	Yapıntı, Turkey	M1/2 (n=1)	1.73	2.1	1.21	1.91	Early Miocene	Bosma et al., 2018
Tamias cf. *eviensis*	Yapıntı, Turkey	M1/2 (n=1)	1.72	2.05	1.19	1.88	Early Miocene	Bosma et al., 2018
Tamias anatoliensis	Altıntas 1, Turkey	M1/2 (n=34)	1.53 (1.41-1.68)	1.93 (1.75-2.06)	1.26	1.72	Late Miocene	Bosma et al., 2013
Tamias anatoliensis	Altıntas 2, Turkey	M1/2 (n=16)	1.53 (1.45-1.62)	1.92 (1.82-2.11)	1.25	1.71	Late Miocene	Bosma et al., 2013
Tamias atsali	Maramena, Turkey	M1/2 (n=9)	1.56 (1.50-1.60)	1.98 (1.92-2.07)	1.27	1.76	Late Miocene	Bosma et al., 2013
Tamias cf. *eviensis*	Karaozu, Turkey	M1/2 (n=1)	1.46	1.81	1.24	1.63	Late Miocene	Bosma et al., 2013
Tamias cf. *eviensis*	Karaozu, Turkey	M1/2 (n=1)	1.51	1.87	1.24	1.68	Late Miocene	Bosma et al., 2013
Tamias cf. *eviensis*	Hayranlı 1, Turkey	M1/2 (n=1)	1.56	1.82	1.17	1.68	Late Miocene	Bosma et al., 2013
Tamias cf. *eviensis*	Hayranlı 1, Turkey	M1/2 (n=1)	1.49	1.8	1.21	1.64	Late Miocene	Bosma et al., 2013
Tamias atsali	Kangal 1, Turkey	M1/2 (n=1)	1.59	1.82	1.14	1.70	Late Miocene	Bosma et al., 2013
Tamias atsali	Kangal 1, Turkey	M1/2 (n=1)	1.54	1.94	1.26	1.73	Late Miocene	Bosma et al., 2013
Tamias urialis	Daud Khel, Pakistan	M1/2 (n=13)	1.35 (1.26- 1.44)	1.71 (1.48-1.80)	1.27	1.52	Middle Miocene	Munthe, 1980
Tamias aff. *atsali*	Suleymanlı 2, Turkey	M1/2 (n=1)	1.41	1.84	1.30	1.61	Late Miocene	Bosma et al., 2013
Tamias urialis	Jalalpur, Pakistan	M1/2 (n=1)	1.5	1.8	1.20	1.64	Late Miocene	Cheema et al., 2000
Tamias urialis	Dehari, Jammu (India)	M1/2 (n=1)	1.3	1.42	1.09	1.36	Middle Miocene	Parmar et al., 2018
Sciurinae gen. et sp. indet.	Jalalpur, Pakistan	M1/2 (n=1)	1.75	2.3	1.31	2.01	Late Miocene	Cheema et al., 2000
Tamias gilaharee	Tappar, Kutch, India	M1/2 (n=1)	1.65	2.1	1.27	1.86	Late Miocene	Patnaik et al., 2022
Tamias urialis	Banda daud Shah (H-GSP 107)	M1/2 (n=1)	1.55	1.88	1.21	1.71	Middle Miocene	Wessels et al., 1982
Tamias urialis	Banda daud Shah (H-GSP 107)	M1/2 (n=1)	1.48	1.92	1.30	1.69	Middle Miocene	Wessels et al., 1982
Tamias urialis	Banda daud Shah (H-GSP 107)	M1/2 (n=1)	1.57	1.76	1.12	1.66	Middle Miocene	Wessels et al., 1982
Sciurinae gen. et sp. indet.	Banda daud Shah (H-GSP 107)	M1 (n=1)	1.81	2.5	1.38	2.13	Middle Miocene	Wessels et al., 1982
cf. *Tamias urialis* (WIMF/A 4731)	Dunera, Punjab, India	M1/M2 (n=1)	1.54	1.87	1.21	1.70	Middle Miocene	This study
Tamias anatoliensis	Altıntas 1, Turkey	m1 (n=14)	1.54 (1.42-1.65)	1.63 (1.47-1.75)	1.06	1.58	Late Miocene	Bosma et al., 2013
Tamias anatoliensis	Altıntas 2, Turkey	m1 (n=11)	1.63 (1.53-1.73)	1.64 (1.55-1.74)	1.01	1.63	Late Miocene	Bosma et al., 2013
Tamias atsali	Maramena, Turkey	m1 (n=7)	1.70 (1.58-1.87)	1.67 (1.54-1.82)	0.98	1.68	Late Miocene	Bosma et al., 2013
Tamias atsali	Kangal 1, Turkey	m1 (n=1)	1.84	1.83	0.99	1.83	Late Miocene	Bosma et al., 2013

TABLE 1 (continued).

Taxon	Locality	Elements (n=sample size)	Mean length (range) in mm	Mean width (range) in mm	Mean width/ length	Square root of width* length	Age	Reference
Tamias atsali	Kangal 1, Turkey	m1 (n=1)	1.72	1.61	0.94	1.66	Late Miocene	Bosma et al., 2013
Tamias atsali	Kangal 1, Turkey	m1 (n=1)	1.49	1.57	1.05	1.53	Late Miocene	Bosma et al., 2013
Tamias atsali	Kangal 1, Turkey	m1 (n=1)	1.61	1.64	1.02	1.62	Late Miocene	Bosma et al., 2013
Tamias aff. *atsali*	Suleymanlı 2, Turkey	m1 (n=1)	1.58	1.44	0.91	1.51	Late Miocene	Bosma et al., 2013
Tamias aff. *atsali*	Suleymanlı 2, Turkey	m1 (n=1)	1.53	1.49	0.97	1.51	Late Miocene	Bosma et al., 2013
Tamias gilaharee	Kutch	m1 (n=1)	1.8	1.7	0.94	1.75	Late Miocene	Patnaik et al., 2022
Tamias anatoliensis	Altıntas 1, Turkey	m2 (n=16)	1.73 (1.47-1.88)	1.77 (1.67-1.90)	1.02	1.75	Late Miocene	Bosma et al., 2013
Tamias anatoliensis	Altıntas 2, Turkey	m2 (n=12)	1.73 (1.51-1.91)	1.76 (1.55-1.94)	1.02	1.74	Late Miocene	Bosma et al., 2013
Tamias atsali	Maramena, Turkey	m2 (n=8)	1.72 (1.54-1.86)	1.81 (1.62-1.90)	1.05	1.76	Late Miocene	Bosma et al., 2013
Tamias atsali	Kangal 1, Turkey	m2 (n=1)	1.71	1.82	1.06	1.76	Late Miocene	Bosma et al., 2013
Tamias atsali	Kangal 1, Turkey	m2 (n=1)	1.85	1.9	1.03	1.87	Late Miocene	Bosma et al., 2013
Tamias atsali	Kangal 1, Turkey	m2 (n=1)	1.51	1.53	1.01	1.52	Late Miocene	Bosma et al., 2013
Tamias aff. *atsali*	Suleymanlı 2, Turkey	m2 (n=1)	1.76	1.72	0.98	1.74	Late Miocene	Bosma et al., 2013
Tamias gilaharee	Kutch	m2 (n=1)	1.57	1.63	1.04	1.60	Late Miocene	Patnaik et al., 2022
Tamias gilaharee	Kutch	m2 (n=1)	1.6	1.45	0.91	1.52	Late Miocene	Patnaik et al., 2022
Tamias cf. *eviensis*	Yapıntı, Turkey	m2 (n=1)	2.08	2.13	1.02	2.10	Early Miocene	Bosma et al., 2018
Tamias cf. *eviensis*	Yapıntı, Turkey	m2 (n=1)	1.85	1.91	1.03	1.88	Early Miocene	Bosma et al., 2018
Tamias cf. *eviensis*	Yapıntı, Turkey	m2 (n=1)	1.91	2.11	1.10	2.01	Early Miocene	Bosma et al., 2018
Tamias urialis	Daud Khel, Pakistan	m1/2 (n=13)	1.42 (1.28-1.56)	1.62 (1.40-1.84)	1.14	1.52	Middle Miocene	Munthe, 1980
Tamias urialis	Banda daud Shah (H-GSP 107)	m1/2 (n=1)	1.68	1.96	1.17	1.81	Middle Miocene	Wessels et al., 1982
Tamias urialis	Banda daud Shah (H-GSP 107)	m1/2 (n=1)	1.56	1.67	1.07	1.61	Middle Miocene	Wessels et al., 1982
Tamias urialis	Banda daud Shah (H-GSP 107)	m1/2 (n=1)	1.46	1.44	0.99	1.45	Middle Miocene	Wessels et al., 1982
Tamias urialis	Banda daud Shah (H-GSP 107)	m1/2 (n=1)	1.55	1.67	1.08	1.61	Middle Miocene	Wessels et al., 1982
cf. *Tamias urialis* (WIMF/A 4749)	Dunera, Punjab, India	m1/m2 (n=1)	1.41	1.5	1.06	1.45	Middle Miocene	This study

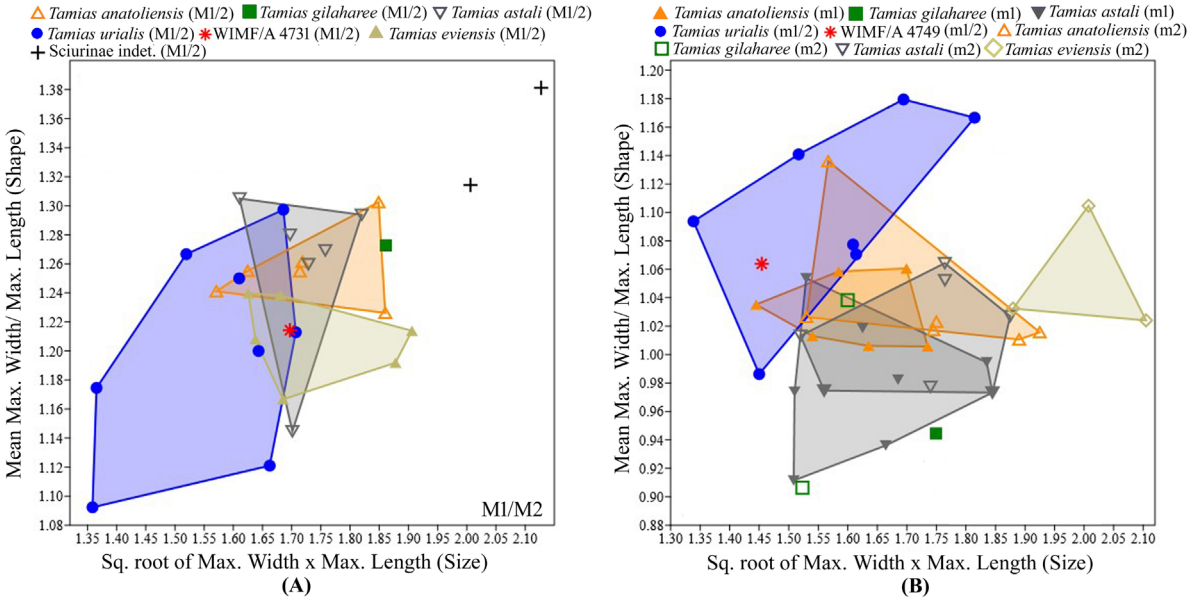

FIGURE 3. Scatterplot of molar size (sq. root of width*length) vs. shape (max. width/length) of Siwalik *Tamias* specimens. A) M1/M2; B) m1/m2. See Table 1 for data used in the plots. Note that minimum, mean and maximum values were used to approximate ranges of variation in large samples of *Tamias anatoliensis*, *T. urialis*, and *T. atsali*.

metaloph with a small metaconule, an indistinct hypocone, and a protoloph often lacking a protoconule.

The m1/2 of *Tamias urialis* is mainly characterized by the presence of three prominent cusps (metaconid, protoconid, and hypoconid), the absence of a mesostylid, entoconid, and mesoconid, a nearly complete metalophid ridge between the metaconid and protoconid, and a sharp ridge connecting the protoconid and hypoconid (Munthe, 1980; Wessels et al., 1982). Overall, the present lower molar (WIMF/A 4749) is similar to the m1/2 of *Tamias urialis* except for its very short and incomplete metalophid. *Tamias gilaharee* m1/2 is characterized by the presence of four main cusps (protoconid, metaconid, hypoconid, and entoconid), a distinct anteroconid, a prominent hypolophid, anterosinusid, mesoconid, and a discontinuous anterolophid. The absence of an entoconid, mesoconid, anteroconid, and mesostylid in WIMF/A 4749 distinguish it from the m1/2 of *Tamias gilaharee*.

WIMF/A 4743 and WIMF/A 4749 are both within the size and shape range for upper and lower first and second molars of the sciurid *Tamias urialis* (see Figure 3A-B). In addition, the observable positions and development of the cusps and crests in the Dunera specimens are also consistent with those previously described for *T. urialis* and distinct from other species of *Tamias*. Therefore, in light of the small sample size, these two specimens from Dunera are most similar to *Tamias urialis*, we tentatively classify them as cf. *Tamias urialis*.

Family CRICETIDAE Fischer von Waldheim, 1817
Genus *DEMOCRICETODON* Fahlbusch, 1969

Type species. *Democricetodon crassus* Fahlbusch, 1969.

Democricetodon fejfari Lindsay, 2017
Figure 4

Holotype. YGSP 19321, left dentary with m1–3.
Type locality. YGSP locality 388, Middle Miocene of Pakistan.
Referred materials. WIMF/A 4734 right M3 (Figure 4A), WIMF/A 4735 left M3 (Figure 4B), WIMF/A 4729 right m1 (Figure 4C); WIMF/A 4740 left m2 (Figure 4D).
Occurrence. Dunera locality, Punjab, India (study area); Middle Miocene Kulwanta (K2) locality, Ramnagar, India; early Late Miocene Tapar locality, Kutch, India; Middle to Late Miocene of Potwar Plateau, Pakistan.
Descriptions. WIMF/A 4734 (Figure 4A) and WIMF/A 4735 (Figure 4B) are both M3s with the mesial cusps and mesial portion of both teeth being much wider than the distal cusps due to strong distal tapering, resulting in a subtriangular occlusal outline. WIMF/A 4734 and 4735 are both broader than long with relatively straight (transversely) mesial margins. The protocone is the largest cusp, followed by the paracone, and the distal

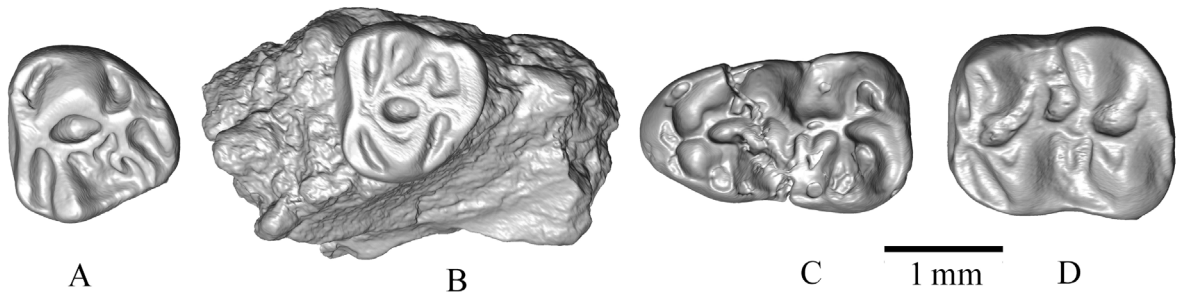

FIGURE 4. 3D surface models of *Democricetodon fejfari* in occlusal views. A) WIMF/A 4734, right M3; B) WIMF/A 4735, left M3; C) WIMF/A 4729, right m1; D) WIMF/A 4740, left m2. Note: Mesial towards the left and distal towards the right in all panels.

cusps are much reduced comparatively. On WIMF/A 4734, a small hypocone is present, and an even smaller metacone can possibly be observed, as well as the mesoloph. On the more worn WIMF/A 4735, the hypocone and metacone are not easily differentiated and appear to have been worn flat. No mesoloph is observable on WIMF/A 4735. The anterior arm of the protocone runs anteriorly towards the midline, connecting with the mesial cingulum near the midline, slightly to the lingual side of the tooth. Similarly, the paracone has an anteriorly directed crest that runs towards the midline of the tooth, meeting the mesial cingulum together with the anterior arm of the protocone. The posterior arm of the protocone is shorter than the anterior arm and is again directed towards the midline of the tooth, connecting distally with the hypocone. In WIMF/A 4734, the hypocone has a posterior crest/arm that connects with the distal cingulum. In WIMF/A 4735, which is more worn, the hypocone and distal cingulum appear indistinct from each other. A mesostyle, ectoloph, and ectostyle are all absent. On the lingual side of the tooth, the anterior cingulum curves posterolingually to terminate near the base of the protocone. On the buccal side of the tooth, the anterior cingulum is relatively long and curves more sharply, posterobuccally, to terminate near the anterior base of the paracone.

WIMF/A 4729 (Figure 4C) is a complete m1. The tooth is relatively long compared to its breadth and tapers mesially (or broadens posteriorly). The mesial border of the tooth is rounded in its outline. The specimen is worn and slightly damaged, making aspects if its morphology difficult to observe. The distal cusps (entoconid and hypoconid) appear larger than the anterior cusps (metaconid and protoconid). The lingual cusps are arranged slightly anterior to the labial cusps, resulting in a slightly offset appearance in occlusal view. The remnants of the anteroconid suggest that it was small and located near the midline on the anterior cingulum. Many of the occlusal crests and features are obscured by wear and/or damage. While the specimen appears most consistent in size and shape with *D. fejfari*, the occlusal details are not well-preserved.

WIMF/A 4740 (Figure 4D) is a relatively complete left m2. In occlusal view the tooth is longer than broad, which leads to an overall rectangular shape. The four main cusps (protoconid, hypoconid, metaconid, and entoconid) appear subequal in size, with the lingual cusps mesially offset from the buccal cusps. In other words, the metaconid is slightly mesial compared to the protoconid, and the entoconid is positioned slightly mesial compared to the hypoconid. The anterior arm of the protoconid is short and merged with the metalophid and the anterolophid near the midline. The posterior arm of the protoconid is also short and directed toward the entoconid, joining the posterior spur of the protoconid and the anterior mure near the midline. The posterior spur of the protoconid is directed lingually and terminates freely. The hypoconid anterior and posterior arms are short, the anterior one merged with posterior mure and the posterior arm merged with posterior cingulum. A short hypolophid and medium-length ectolophid are present. Mesolophid, mesostylid, and ectostylid are absent. The entolophid is directed buccally from the entoconid to join the anterior arm of the hypoconid near the midline of the tooth. The anterobuccal cingulum is high and curves posteriorly to terminate near the base of the protoconid. The anterolingual cingulum is also high, but it is very short and terminates on the anterior side of the metaconid. The tooth's lingual shelf is slightly deeper than its labial shelf. The posterior cingulum is long and high, curves

anteriorly, and partially encloses a shallow posterolingual basin.

Comparison and Remarks. The Siwalik Miocene Cricetidae are generally represented by two major taxonomic groups: *Democricetodon* and *Megacricetodon* (Fahlbusch, 1964; Lindsay, 2017). *Democricetodon* molars differ from *Megacricetodon* by sometimes possessing two lophs, i.e., thin crests that are directed buccally between the paracone and metacone in upper teeth, or two lophids, similar crests that are directed lingually between the metaconid and entoconid in lower teeth (Lindsay, 2017). All the cricetid specimens recovered from Dunera are here identified as *Democricetodon* by having two lophids between the metaconid and entoconid on m1 and m2, and a short mesoloph on M3.

In the Siwalik deposits of the Indian subcontinent, five species of *Democricetodon* are recognized: *D. kohatensis* Wessels et al., 1982, *D. fejfari* Lindsay, 2017, and three smaller and unnamed species (*Democricetodon* sp. A; *Democricetodon* sp. B-C; and *Democricetodon* sp. D). Because they are found in older Siwalik deposits ~18 Ma, Lindsay (2017) suggested that the three smaller unnamed species might have evolved prior to their first recorded appearance, before the deposition of the Siwalik deposits in Pakistan. The last recorded species of *Democricetodon* is *D. fejfari* at ~8.7 Ma in the Siwalik deposits of Pakistan, and the first appearance of *D. fejfari* is ~13.8 Ma, which is also about the same time as the appearance of *Antemus* (Lindsay, 2017). The Early Miocene species *D. khani* was reported from the Murree Formation of Banda Daud Shah, Chitarwata Formation, and Vihowa Formation of Pakistan (de Bruijn et al., 1981).

Compared to the known species of *Democricetodon*, the present m1 correlates well with the early Miocene species *D. khani* by having an extra transverse crest (protoconid posterior spur) between the metaconid and entoconid that is distinct from a true mesolophid, but differs from *D. khani* in its large size and sharp anterolophid. Among the Siwalik species of *Democricetodon*, the recovered m1 is very similar to *D. fejfari.* Recently, *D. fejfari* was also reported from the Middle Miocene K2 (Kulwanta) locality near Ramnagar, India (Parmar et al., 2022) and the Late Miocene of Gujarat, India (Bhandari et al., 2021; Patnaik et al., 2022). The m1 of *D. fejfari* is characterized by its relatively large size, small and single-cusped anteroconid, more offset lingual cusps that are mesially positioned compared to the labial cusps, lingually flexed posterior arm of the protoconid (resembling the mesolophid) directed toward the lingual margin of the tooth, and a short mesolophid (Lindsay, 2017). These features are present in the m1 described here and hence suggest assignment of WIMF/A 4729 to *D. fejfari*.

The present m2 is also comparable to *D. fejfari* and *D. khani* by the presence of the protoconid posterior spur (loph near the protocone), but the ectolophid on this tooth differs from that in *D. khani*. The m2 WIMF/A 4740 (length=1.88 and width=1.57 mm) is also much larger in size than the m2 of *D. khani* (length=1.2 mm and width=0.98 mm reported in Lindsay and Flynn, 2016), and generally falls towards the larger size range for *D. fejfari*, particularly in length (Lindsay, 2017).

The Dunera M3 is similar to *D. khani* in possessing a subtriangular outline, a large protocone (larger than the other major cusps), and a prominent anterior cingulum (Lindsay and Flynn, 2016). However, the Dunera M3 displays an indistinct metacone, which is typically distinct in *D. khani* from the early Miocene. Another distinct feature found in *D. khani* is the presence of two lophs (mesoloph and protocone posterior spur) in M3, whereas the Dunera M3 displays only one loph. While the protocone posterior spur is difficult to distinguish from the mesoloph in many rodent teeth, Lindsay and Flynn (2016) clarified that a loph close to the paracone should be recognized as the protocone posterior spur, and the loph close to the metacone should be recognized as the mesoloph. Because the Dunera specimen exhibits one loph that is close to the paracone, this loph represents the protocone posterior spur. Thus, the Dunera M3 is clearly distinguished from *D. kohatensis*, which instead displays a well-developed mesoloph, long anteroloph, and small size (Wessels et al., 1982). The present M3 closely resembles the M3 of *D. fejfari* (Lindsay, 2017) in its triangular outline, larger protocone, prominent anterior cingulum, and the presence of the protocone posterior spur.

When the size and shape of the Dunera specimens are compared to other described species of *Democricetodon* from the Siwaliks and Asia, more broadly (Cheema et al., 2000; Wessels and Reumer, 2009; Zhu-Ding, 2010; Lindsay and Flynn, 2016; Lindsay, 2017; Patnaik et al., 2022), the m1, m2, and M3 described here fall within the size range of *D. fejfari* but the shape of the Dunera m1 is slightly narrower than other *D. feifari* specimens (see Table 2). However, they are otherwise morphologically similar to *D. fejfari*, and we assign them to this species at this time.

TABLE 2. Comparison of Dunera *Democricetodon* with other *Democricetodon* from Siwaliks and Asia.

Taxon	Locality	Elements (n=sample size)	Mean length (range) in mm	Mean width (range) in mm	Mean width/ length	Square root of width* length	Age	Reference
Democricetodon fejfari	Tappar, Kutch, India	m1 (n=2)	1.88	1.98	1.05	1.93	Late Miocene (11- 10 Ma)	Patnaik et al., 2022
Democricetodon suensis	China	m1 (n=29)	1.43 (1.25-1.60)	1.05 (0.90-1.15)	0.73	1.23	Early Miocene	Zhu-Ding, 2010
Democricetodon sui	China	m1 (n=5)	1.26 (1.20-1.31)	0.84 (0.80-0.91)	0.67	1.03	Early Miocene	Maridet et al., 2011
Democricetodon fejfari	Pakistan	m1 (n=18)	1.89 (1.03-2.13)	1.32 (0.96-1.56)	0.70	1.58	Middle to Late Miocene (13-8.7 Ma)	Lindsay, 2017
Democricetodon gracilis	Germany	m1 (n=141)	1.30 (1.12-1.43)	0.91 (0.78-1)	0.70	1.09	Middle Miocene (16 Ma)	Wessels and Reumer, 2009
Democricetodon mutulus	Germany	m1 (n=182)	1.67 (1.48-1.86)	1.11 (0.99-1.24)	0.66	1.36	Middle Miocene (16 Ma)	Wessels and Reumer, 2009
Democricetodon kohatensis	Pakistan	m1 (n=3)	1.50 (1.40-1.60)	1.17 (1.15-1.20)	0.78	1.32	Late Miocene (11-10 Ma)	Cheema et al., 2000
Democricetodon khani	Pakistan	m1 (n=1)	1.42	1	0.70	1.19	Early Miocene (19 Ma)	Lindsay and Flynn, 2016
Democricetodon sp. B-C	Pakistan	m1 (n=1)	2.05	1.3	0.63	1.63	Late Miocene (11-10 Ma)	Cheema et al., 2000
Democricetodon sp. G	Pakistan	m1 (n=1)	1.95	1.3	0.67	1.59	Late Miocene (11- 10 Ma)	Cheema et al., 2000
Democricetodon fejfari	Dunera, Punjab, India	m1 (n=1)	2.3	1.37	0.60	1.78	Late Miocene (11-10 Ma)	This study
Democricetodon fejfari	Tappar, Kutch, India	m2 (n=7)	1.35 (1.25-1.45)	1.06 (1.00-1.13)	0.79	1.20	Late Miocene (11-10 Ma)	Patnaik et al., 2022
Democricetodon suensis	China	m2 (n=38)	1.36 (1.20-1.50)	1.12 (1.00-1.20)	0.82	1.23	Early Miocene	Zhu-Ding, 2010
Democricetodon gracilis	Germany	m2 (n=156)	1.18 (1.06-1.28)	0.98 (0.9-1.15)	0.83	1.08	Middle Miocene (16 Ma)	Wessels and Reumer, 2009
Democricetodon fejfari	Pakistan	m2 (n=33)	1.65 (1.14-1.88)	1.42 (0.98-1.72)	0.86	1.53	Middle to Late Miocene (13-8.7 Ma)	Lindsay, 2017
Democricetodon mutulus	Grmany	m2 (n=217)	1.52 (1.37-1.68)	1.24 (1.10-1.39)	0.82	1.37	Middle Miocene (16 Ma)	Wessels and Reumer, 2009
Democricetodon kohatensis	Pakistan	m2 (n=2)	1.42 (1.40-1.45)	1.17 (1.15-1.20)	0.82	1.29	Late Miocene (11-10 Ma)	Cheema et al., 2000
Democricetodon khani	Pakistan	m2 (n=1)	1.21	0.98	0.81	1.09	Early Miocene (19 Ma)	Lindsay and Flynn, 2016
Democricetodon sp. B-C	Pakistan	m2 (n=1)	1.7	1.6	0.94	1.65	Late Miocene (11-10 Ma)	Cheema et al., 2000
Democricetodon sp. G	Pakistan	m2 (n=1)	1.75	1.65	0.94	1.70	Late Miocene (11- 10 Ma)	Cheema et al., 2000
Democricetodon fejfari	Dunera	m2 (n=1)	1.88	1.57	0.84	1.72	Late Miocene (11-10 Ma)	This study
Democricetodon gracilis	Germany	M3 (n=80)	0.84 (0.70-0.94)	0.89 (0.77-0.98)	1.06	0.86	Middle Miocene (16 Ma)	Wessels and Reumer, 2009

TABLE 2 (continued).

Taxon	Locality	Elements (n=sample size)	Mean length (range) in mm	Mean width (range) in mm	Mean width/ length	Square root of width* length	Age	Reference
Democricetodon mutulus	Germany	M3 (n=122)	1.09 (0.98-1.23)	1.13 (1.05-1.24)	1.04	1.11	Middle Miocene (16 Ma)	Wessels and Reumer, 2009
Democricetodon khani	Pakistan	M3 (n=1)	0.95	1.09	1.15	1.02	Early Miocene (19 Ma)	Lindsay and Flynn, 2016
Democricetodon suensis	China	M3 (n=11)	1.06 (1.00-1.15)	1.08 (1.00-1.15)	1.02	1.07	Early Miocene	Zhu-Ding, 2010
Democricetodon sui	China	M3 (n=1)	0.68	0.93	1.37	0.80	Early Miocene	Maridet et al., 2011
Democricetodon fejfari	Pakistan	M3 (n=3)	1.55 (1.30-2.03)	1.43 (1.40-1.47)	0.92	1.49	Middle to Late Miocene (13-8.7 Ma)	Lindsay, 2017
Democricetodon fejfari	Tappar, Kutch, India	M3 (n=1)	0.99	1	1.01	0.99	Late Miocene (11-10 ma)	Patnaik et al., 2022
Democricetodon kohatensis	Pakistan	M3 (n=1)	1.05	1.15	1.10	1.10	Late Miocene (11-10 Ma)	Cheema et al., 2000
Democricetodon sp. B-C	Pakistan	M3 (n=1)	1.2	1.35	1.13	1.27	Late Miocene (11-10 Ma)	Cheema et al., 2000
Democricetodon sp. G	Pakistan	M3 (n=2)	1.32 (1.30-1.35)	1.47 (1.45-1.50)	1.11	1.39	Late Miocene (11-10 Ma)	Cheema et al., 2000
Democricetodon fejfari	Dunera, Punjab, India	M3 (n=2)	1.4 (1.33-1.47)	1.41 (1.34-1.49)	1.01	1.40	Late Miocene (11-10 Ma)	This study

Family MURIDAE Illiger, 1811
Subfamily MURINAE illiger, 1811
Genus *PROGONOMYS* Schaub, 1938

Type species. *Progonomys cathalai* Schaub, 1938.

Progonomys cf. *hussaini* Cheema et al., 2000
Figure 5A-H

Holotype. PMNH 5062, left M1.

Type locality. JAL-101, upper portion of the Chinji Formation of the Jalalpur area, Chakwal District, Potwar Plateau, Pakistan.

Referred materials. WIMF/A 4745 right M1 (Figure 5A), WIMF/A 4746 left M2 (Figure 5B), WIMF/A 4747 left M2 (Figure 5C), WIMF/A 4739 right m1 (Figure 5D), WIMF/A 4737 left m2 (Figure 5E), WIMF/A 4738 left m2 (Figure 5F), WIMF/A 4748 left m2 (Figure 5G), WIMF/A 4736 right m3 (Figure 5H).

Occurrence. Dunera locality, Punjab, India (study area); early Late Miocene of Potwar Plateau, Pakistan.

Description. WIMF/A 4745 (Figure 5A) is a right M1 with three roots that is slightly damaged on its buccal side. In occlusal view, the t1 (anterostyle) is placed posterolingually in relation to t2 (lingual anterocone) and t3 (labial anterocone), and weakly connected to the t2. The measured angle between the t1 and the longitudinal axis passing through the centre of the tooth (angle of anterostyle) is ~45°. The t2 and t3 are similar in size. The t4 (enterostyle) is also placed posteriorly compared to t5 (protocone), but is similar in mesiodistal position to t6 (paracone). The enterostyle is weakly connected to t5 (a characteristic that was determined after digitally removing matrix on the occlusal surface) and the measured angle of the enterostyle (angle formed by protocone and enterostyle) is ~72°. The larger t8 (hypocone) is attached to the smaller t9 (metacone). Overall, the cusps are inclined posteriorly and relatively weakly connected transversely. The precingulum is well developed at the mesial end of the tooth and bears a cuspule on its anterolabial margin. The small ridge-like posterior cingulum is connected to the t8, but also separated from it by a small sinus. The t1 and t4 are positioned posteriorly, and laterally compressed and elongated.

The M2s, WIMF/A 4746 (Figure 5B) and 4747 (Figure 5C), are trapezoidal in occlusal outline. The

enterostyle is posterolingual to the protocone and connected to the protocone by a small crest in WIMF/A 4747. In WIMF/A 4746, the potential connection between the enterostyle and protocone is weak. In both specimens, the enterostyle is similar or slightly smaller in size compared to the protocone. The protocone is larger than the paracone, and it is connected by a short crest. An anterostyle is present at the mesiolingual corner of each tooth, continuous with the anterior cingulum. The buccal anterostyle is located just mesial to the paracone and is a small button-shaped cusp in WIMF/A 4747 but more flattened in WIMF/A 4746. On the posterior chevron, a large hypocone is present, connected to the much smaller metacone by a mesiobuccally oriented crest. The hypocone is the largest cusp on both specimens, and the metacone is the smallest. The posterior cingulum is connected to the hypocone but isolated from the metacone by a shallow groove. All cusps are gently inclined posteriorly, and both teeth have three roots.

WIMF/A 4739 (Figure 5D) is a right m1 and heavily worn, particularly on its lingual side. Its prelobe comprises a labial anteroconid and the remnants of a lingual anteroconid, with the larger labial anteroconid placed slightly distal compared to the lingual anteroconid. The pre-lobe (lingual and labial anteroconids) and the second lobe (protoconid and metaconid) form an “X” shape with a weak longitudinal connection placed towards the lingual side of the tooth, presumably an artifact of the lingual wear. The cuspids of the second lobe, the protoconid and the metaconid, are strongly connected with the protoconid larger and better preserved. The cuspids of the third lobe also have a strong transverse connection, with the buccal cusp (hypoconid) again better preserved compared to the lingual cusp (entoconid). Due in part to the wear on the lingual side, the buccal cusps appear larger and slightly distal relative to the lingual cusps. A buccal cingulum is present, along with prominent C1 and C3 cingular cusps. The posterior cingulum is short and placed towards the lingual side of the tooth; it does not connect to the buccal cingulum. The specimen has two roots.

WIMF/A 4737 (Figure 5E), WIMF/A 4738 (Figure 5F) and WIMF/A 4748 (Figure 5G) are left m2s. The teeth are rectangular to trapezoidal in outline, tapering distally. The protoconid and metaconid are

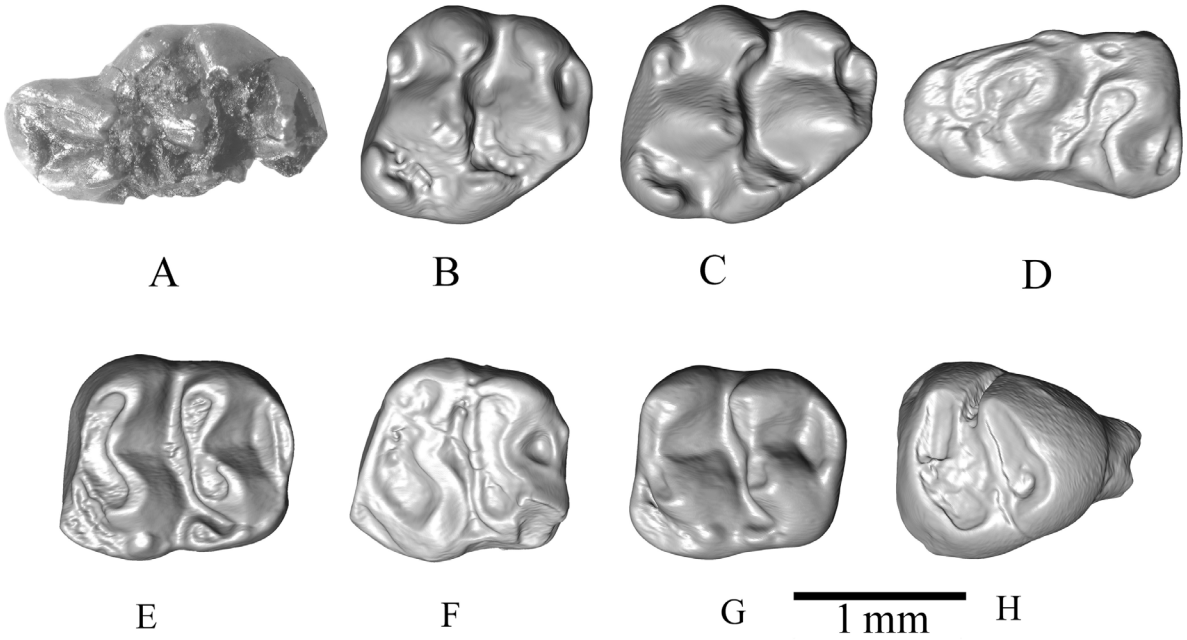

FIGURE 5. *Progonomys* cf. *hussaini* in occlusal views. Leica stereozoom Microscope image: A) WIMF/A 4745, right M1. 3D surface models: B) WIMF/A 4746, left M2; C) WIMF/A 4747, left M2; D) WIMF/A 4739, right m1; E) WIMF/A 4737, left m2; F) WIMF/A 4738, left m2; G) WIMF/A 4748, left m2; H) WIMF/A 4736, right m3. Note: Mesial towards the left and distal towards the right in all panels.

strongly connected to form the first chevron, whereas the hypoconid and entoconid are connected by a narrower crest and form the second chevron. All three specimens appear to display a labial anteroconid in the mesiobuccal corner of the tooth, particularly visible in the less worn WIMF/A 4737 and WIMF/A 4748 specimens. WIMF/A 4738 is heavily worn compared to the other two teeth, and thus the chevrons appear relatively larger in this specimen. In all three m2s, the first and second chevrons form a distally curving gentle arc, with the second chevron being more transverse (i.e., straight) compared to the first chevron. In both chevrons, the buccal cusps (protoconid and hypoconid) are slightly distal compared to the lingual cusps. In the two relatively unworn/lightly worn specimens (WIMF/A 4737 and 4748), a buccal cingulum is present with an accessory cuspid (C1) connected to the protoconid. In WIMF/A 4738, the C1 does not appear to be present (Figure 5F). A posterior cingulum is present between the hypoconid and entoconid at the distal end of all three molars. The m2s have two roots.

WIMF/A 4736 (Figure 5H) is a left m3 with a relatively triangular-shaped outline owing to its strong distal tapering. The anterior portion is slightly eroded, but the remnants of a labial anteroconid is present on the remaining anterior cingulum. The protoconid and the metaconid are strongly connected. The protoconid is distally positioned compared to the metaconid. The hypoconid is connected to the entoconid to form the distal cusp row, and like the anterior chevron, the buccal cusp (hypconid) is slightly distal to the lingual cusp (entoconid). There is no buccal or posterior cingulum. There are no accessory cusps on the tooth and it has two roots.

Comparison and Remarks. The Dunera murine M1 and m1 differ from those of *Antemus* in the presence of a connection between the t4/enterostyle with the protocone on M1 and an asymmetrical 'X' shaped longitudinal connection between the first and second chevrons on m1. The Dunera m2 differs from those of *Antemus* in having a strong connection between the cusps, and the molars generally display gently, posteriorly inclined cusps, another more advanced feature compared to *Antemus*. The presence of a large anteroposteriorly compressed and elongated anterostyle (t1) on the Dunera M1 (visible on the CT scan with the matrix removed), and the small size of the Dunera specimens in general, also differs from that of typical *Karnimata*.

These new Dunera specimens share most features with *Progonomys*, including an M1 with an enterostyle connected to the protocone, posteriorly inclined cusps, a posteriorly shifted t1/anterostyle, and a well-defined posterior cingulum; an m1 with twinned anteroconids, an asymmetrical 'X' shaped longitudinal connection, a relatively well-developed (but worn) buccal cingulum, and accessory cusps C1 and C3 on the buccal cingulum. By looking at the angle of enterostyle and the angle of anterostyle among murines, the enterostyle angle on the present M1 is within the range of numerous murine species including pre-*Progonomys* and *P. hussaini*, but outside the range of *Progonomys* species that are known from ~9.2 Ma and younger horizons. The measured angle of anterostyle in the Dunera M1 is greater than *Antemus chinjiensis, Progonomys debruijni,* and pre-*Progonomys*, but is within the range of *P. hussaini* (see the angle measurements in Kimura et al., 2013, 2021). However, the enterostyle/t4 on M1 and M2 is weakly connected to the protocone unlike the strong connection in many species of *Progonomys.* If all of the described specimens belong to a single species, they are most similar to those described as *Progonomys hussaini* (Cheema at al., 2000) or "pre-*Progonomys*" (Flynn et al., 2020). However, the m3 (WIMF/A 4736) is notable for its apparently large size, larger than all other measured *Antemus*, *Progonomys*, and *Karnimata* specimens in our sample (Figure 6; Appendix). Therefore, it is quite possible that more than one species is represented among the murine sample from Dunera.

The Dunera specimens differ from *Progonomys morganae* (Kimura et al., 2017) and *Progonomys debruijni* (Jacobs, 1978) in having a strong precingulum on M1 and strongly appressed anteroconids forming one lobe connected weakly to the second lobe lingually on m1. The present specimens also differ from *Progonomys prasadi*, a new species described by Patnaik et al. (2022) from the Late Miocene of Kutch, in its smaller size (for all teeth other than m3), having M1 with cusps weakly connected transversely, an m1 with a short posterior cingulum, and an m3 with the lack of C1. In overall size and shape, the specimens overlap with specimens assigned to species of *Antemus* and *Progonomys,* falling closest to the mean of *P. hussaini* or "pre-*Progonomys*" in most comparisons (Figure 6; Appendix).

The known time-range of *P. hussaini* and "pre-*Progonomys*" across sites in Pakistan spans a time period of ~11.6-10 Ma (Cheema et al., 2000; Flynn et al., 2020; Kimura et al., 2021). This time range

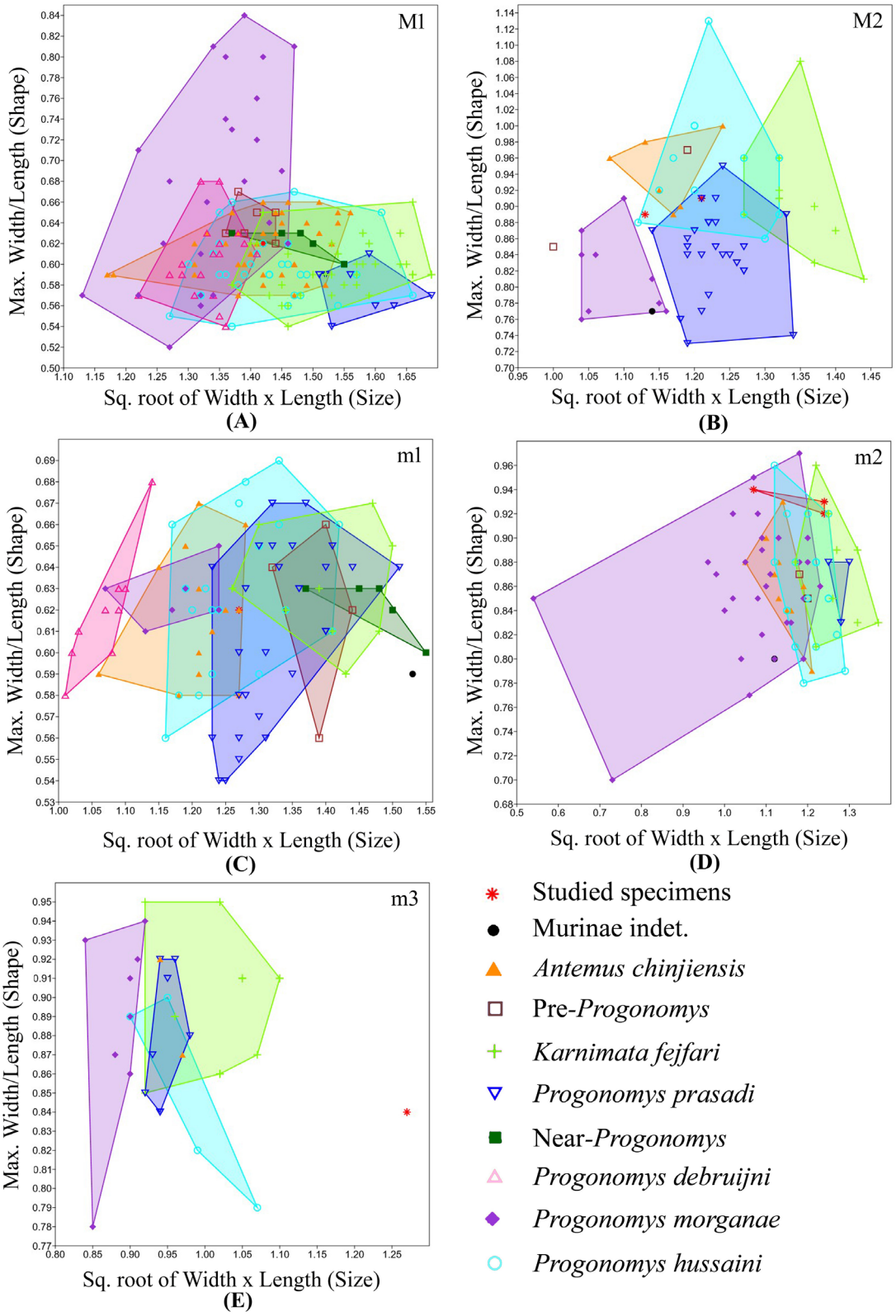

FIGURE 6. Scatterplot of molar size (sq. root of width*length) vs. shape (max. width/length) in Siwalik murid specimens. A) M1; B) M2; C) m1; D) m2; E) m3. See Appendix for data used in the plots.

accords well with previous paleomagnetic data from Dunera, which records normal polarity and has been correlated to the long C5n chron, ~11.06-9.8 Ma (Cande and Kent, 1995; Sinha et al., 2005; Ogg, 2020). Currently, we assign these specimens to *Progonomys* cf. *hussaini*, given that they seem most similar to *P. hussaini* and yet are placed near the bottom of the C5n chron, close to ~11 Ma and ~500 thousand years earlier than the FAD for *P. hussaini* in Pakistan (Kimura et al., 2021). Because there is a time gap in major micromammal sites on the Potwar Plateau between ~11.1 Ma and 10.5 Ma (Kimura et al., 2021), it is quite possible that Dunera helps to fill in this gap and samples an earlier population of *P. hussaini* or a transitional stage between pre-*Progonomys* and *P. hussaini*. A biochronological estimate up to ~11 Ma (between ~11-10 Ma) was previously suggested for the type series of *P. hussaini* from locality JAL-101 in the Chinji Formation (Cheema et al., 2000). If the older age estimate for JAL-101 is correct, it may be coeval with Dunera and also sample the same time gap. Additional M1 specimens could help confirm this assignment, but if confirmed, the Dunera specimens perhaps represent a new FAD for the *P. hussaini* lineage.

Family CTENODACTYLIDAE Zittel, 1893
Genus *SAYIMYS* Wood, 1937

Type species. *Sayimys perplexus* Wood, 1937

Sayimys sivalensis (Hinton, 1933)
Figure 7

Holotype. GSI D284, left partial dentary with m2–m3.

Type locality. Chinji village, Middle Miocene of Pakistan.

Referred materials. WIMF/A 4733 left M2 (Figure 7A), WIMF/A 4750 right M2 (Figure 7B), WIMF/A 4731 left M2 or M3 (Figure 7C); WIMF/A 4732 left m1 or m2 (Figure 7D).

Occurrence. Dunera locality, Punjab, India (study area), early Late Miocene Tapar locality, Kutch, India; Middle Miocene Dehari locality, Ramnagar, India; Late Miocene Haritalyangar locality, India; Middle Miocene, Sind, Pakistan; Middle to Late Miocene of Potwar Plateau, Pakistan.

Description. WIMF/A 4733 (Figure 7A) is identified as a likely M2 based in part on its size, which is larger than any M1 described for *S. sivalensis* by Munthe (1980). In occlusal view, the tooth narrows distally, and the outline of the mesial occlusal surface is rounded while the distal end is squared off. The lingual cusps (protocone and hypocone) are larger than the buccal cusps (paracone and metacone). The protocone is somewhat larger and extends more lingually than the hypocone. The paraflexus is indistinct, if present, with a slight indentation just anterior to the paracone. The mesoflexus is wider and greater in depth than hypoflexus, and these features are oriented slightly oblique to each other, separated by a small, narrow crest running mesiodistally on the lingual side of the tooth, connecting the anteroloph to the metaloph/posteroloph. A short metaflexus is present just distal to the metacone, and the posteroloph is shorter than the metaloph.

WIMF/A 4750 (Figure 7B) is also identified as a likely M2, again based in part on its size, which is larger than M1s described by Munthe (1980) as well as slightly larger than WIMF/A 4733. In overall

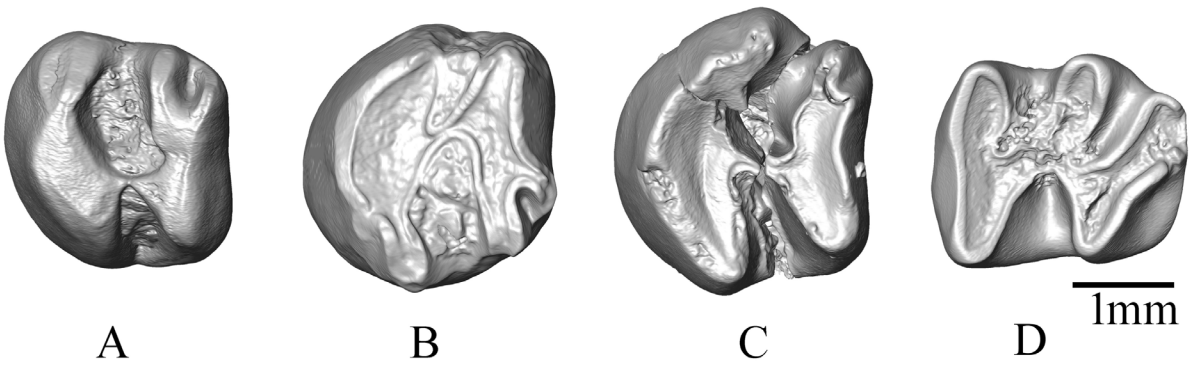

FIGURE 7. 3D surface models of *Sayimys sivalensis* in occlusal views. A) WIMF/A 4733, left M2; B) WIMF/A 4750, right M2 C) WIMF/A 4731, left M2 or M3; D) WIMF/A 4732 left m1 or m2. Note: Mesial towards the left and distal towards the right in all panels.

shape, WIMF/A 4750 is similar to WIMF/A 4733 with the distal portion of the tooth narrower than the mesial portion in occlusal view. WIMF/A 4750 is more worn than WIMF/A 4733, perhaps accounting for some of the minor differences between the teeth. The lingual cusps are again larger than the buccal cusps, with the protocone larger than the hypocone. Both lingual cusps extend to the lingual border of the tootha and neither cusp appears to extend more lingually than the other. The paraflexus is indistinct, with the slightest hint of an indentation or facet present just anterior to the paracone, although some of this appearance could be due to slight damage and wear. The mesoflexus is wider and greater in depth than hypoflexus, with the mesoflexus oriented lingually and the hypoflexus narrower and oriented mesiobuccally. The mesoflexus and hypoflexus are separated by a tiny, narrow crest running mesiodistally and slightly distolingually on the lingual side of the tooth, connecting the anteroloph to the metaloph/posteroloph. A short metaflexus is present just distal to the metacone, and a very short posteroloph is present (shorter than the metaloph) and oriented distobuccally, but more distally oriented compared to the posteroloph in WIMF/A 4733.

WIMF/A 4731 (Figure 7C) is a left M2 or M3, most likely an M3. Though slightly larger, it is morphologically similar to the above described M2s. The paraflexus appears absent, with only the slightest indentation anterior to the paracone. The protocone is slightly larger than the hypocone, and the tooth narrows distally, to a greater degree than seen in the M2s. The mesoflexus and hypoflexus are more equal in size depth compared to the M2s, although the mesoflexus is still larger. They both terminate opposite each other near the midline, separated by a narrow mesiodistally oriented crest connecting the anteroloph to the metaloph/posteroloph. An extremely short metaflexus is present, represented by a shallow indentation distal to the metacone.

WIMF/A 4732 (Figure 7D) is most probably a left m2 based on its relatively large size but given that m1 and m2 are difficult to separate morphologically, we describe it as an m1 or an m2. The occlusal outline of the tooth is sub-rectangular, slightly narrower posteriorly, with a transversely straight anterior margin that slightly narrows posteriorly. The protoconid is ‘v’ shaped and its anterior arm connects to the metalophid terminating at the metaconid. The protoconid extends more buccally compared to the hypoconid. The mesoflexid is slightly shorter and deeper than the metaflexid. The hypolophid runs at a slightly oblique angle postero-lingually, terminating at entoconid. The hypoconid is also ‘v’ shaped and its posterior arm merges with the obliquely oriented posterolophid that runs almost parallel to the hypolophid. The connection of the anterior arm of the hypoconid with the hypolophid is narrow, meeting near the midline of the tooth. The hypoflexid is much larger and deeper compared to the mesoflexid and metaflexid.

Comparison and Remarks. Five ctenodactylid species belonging to two genera, *Prosayimys* and *Sayimys*, are currently recognized from the Neogene of the Indian subcontinent (López-Antoñanzas and Sen, 2003; López-Antoñanzas and Knoll, 2011). *Prosayimys flynni* is found in the Early Miocene Chitarwata Formation of Zinda Pir Dome, Pakistan, and at least four species of *Sayimys* are recognized at many Neogene sites across India and Pakistan (López-Antoñanzas and Sen, 2003; López-Antoñanzas and Knoll, 2011). The present specimens are very similar to those of the long ranging (Middle Miocene-Late Miocene) form *S. sivalensis* in having derived characters such as: semi-hypsodont teeth, a mesoflexid almost equal to the metaflexid in length on m1-m2, and a short or absent paraflexus and metaflexus on M1/M2 and M3. The present described specimens are larger in size compared to many species of *Sayimys* from the Siwaliks but fall within the range of *Sayimys sivalensis* (*sensu* López-Antoñanzas and Sen, 2003, including *S. perplexus* and *S. chinjiensis*), further supporting their assignment to *S. sivalensis* (see Table 3).

DISCUSSION

Dunera is a small town in Pathankot District of Punjab State, India. Vasishat et al. (1983) reported a few large mammals (i.e., *Dorcatherium* sp., *Giraffokeryx* sp. and an indeterminate bovid) from a locality exposed close to Dunera, but since then no additional mammalian fossils have been reported from this area. Recently, we have found a diverse small mammal assemblage from the same locality. The micromammal material described here are identified as the murine *Progonomys* cf. *hussaini*, the ctenodactylid *Sayimys sivalenis*, the cricetid *Democricetodon fejfari*, and the sciurid cf. *Tamias urialis*, all of which are documented for the first time from this area.

In the Siwaliks of the Indian subcontinent, a high resolution biochronological framework has been established, particularly between ~18 to 5 Ma, by integrating magnetic polarity stratigraphy,

TABLE 3. Comparative dental measurements (mm) of Dunera *Sayimys* and other *Sayimys* specimens from Indian subcontinent.

Taxon	Locality	Elements (sample size)	Mean length (range) in mm	Mean width (range) in mm	Mean width/ length	Square root of width* Length	Mean ant./ mean Post.	Geological Formation	Reference
Sayimys sivalensis (including *S. chinjiensis*)	Potwar Plateau, Pakistan	M1/M2 (L=55; W=53,55)	1.94 (1.60-2.52)	Ant: 2.05 (1.65-2.65) Post: 1.91 (1.50-2.45)	1.06	1.99	1.07	Kamlial, Chinji, and Nagri	Baskin, 1996; López-Antoñanzas & Sen, 2003
Sayimys sivalensis (including *S. chinjiensis*)	Potwar Plateau, Pakistan	M3 (L=12; W=11,12)	2.25 (1.72-2.52)	Ant: 2.47 (2.08-2.80) Post: 2.08 (1.55-2.40)	1.10	2.36	1.19	Kamlial, Chinji, and Nagri	Baskin, 1996
Sayimys sivalensis	Daud Khel, Potwar Plateau, Pakistan	M1 (L=29, W=29,29)	2.08 (1.84-2.24)	Ant: 2.02 (1.68-2.36) Post: 1.92 (1.68-2.20)	0.97	2.05	1.05	Chinji	Munthe, 1980
Sayimys sivalensis	Daud Khel, Potwar Plateau, Pakistan	M2 (L=31, W=31,31)	2.33 (1.96-2.60)	Ant: 2.46 (2.12-2.80) Post: 2.20 (1.92-2.56)	1.06	2.39	1.12	Chinji	Munthe, 1980
Sayimys sivalensis	Daud Khel, Potwar Plateau, Pakistan	M3 (L=21; W=21,21)	2.28 (1.96-2.64)	Ant: 2.50 (2.28-2.72) Post: 1.77 (1.56-1.96)	1.10	2.39	1.41	Chinji	Munthe, 1980
Sayimys sivalensis	Dunera (Punjab), India	M3	2.48	Ant: 2.83 Post: 2.35	1.14	2.65	1.20	Nagri Age	This study
Sayimys sivalensis	Dunera (Punjab), India	M1/M2	2.44 (2.4-2.48)	Ant: 2.44 (2.35-2.53) Post: 2.20 (2.20-2.21)	1.00	2.44	1.11	Nagri Age	This study
Sayimys sivalensis WIMF/A 4695	Ramnagar (Dehari 2), India	M2 or M3	2.25	Ant:2.41 Post: 2.02	1.07	2.33	1.19	Chinji	Sehgal et al., 2022
Sayimys sivalensis PUCT5	Kutch	M1/M2	1.8	Ant:2.00 Post: 1.82	1.11	1.90	1.10	Late Miocene (=Nagri)	Patnaik et al., 2022
Sayimys sivalensis PUCT 4	Kutch	M3	2.15	Ant: 2.25 Post: 1.54	1.05	2.20	1.46	Late Miocene (=Nagri)	Patnaik et al., 2022
Sayimys cf. *S. intermedius*	Zinda Pir Dome and Potwar Plateau, Pakistan	M1/M2 (L=6; W=4,5)	1.97 (1.78-2.22)	Ant: 2.15 (2.10-2.20) Post: 1.94 (1.82-2.08)	1.09	2.06	1.11	Vihowa and Kamlial	Baskin, 1996
Sayimys cf. *S. intermedius*	Zinda Pir Dome, Vihowa Fm. and Kamlial Fm., Potwar Plateau, Pakistan	M3 (L=2; W=2,4)	1.96 (1.80-2.12)	Ant: 2.04 (1.95-2.12) Post: 1.68 (1.60-1.75)	1.04	2.00	1.22	Vihowa and Kamlial	Baskin, 1996
Sayimysbaskini (=Sayimys cf. *S. minor)*	YGSP721, Potwar Plateau, Pakistan	M1/M2 (L=7; W=5,5)	1.52 (1.32-1.62)	Ant: 1.49 (1.32-1.60) Post: 1.46 (1.30-1.55)	0.98	1.50	1.02	Kamlial	Baskin, 1996
Sayimysbaskini (=Sayimys cf. *S. minor)*	YGSP721 Pakistan	M3 (L=X; W=X,1)	-	Post: 1.62	-	-	-	Kamlial	Baskin, 1996
Sayimysbaskini (=Sayimys cf. *S. minor)*	YGSP747 Pakistan	M1/M2 (L=9; W=7,6)	1.69 (1.57-1.85)	Ant: 1.94 (1.60-2.25) Post: 1.73 (1.57-2.13)	1.15	1.81	1.12	Kamlial	Baskin, 1996
Sayimysbaskini (=Sayimys cf. *S. minor)*	YGSP747 Pakistan	M3 (L=1; W=1,1)	1.75	Ant:2.00 Post: 1.85	1.14	1.87	1.08	Kamlial	Baskin, 1996
Sayamis sivalensis	Dunera (Punjab), India	m1/m2	2.43	Ant:2.06 Post: 2.04	0.85	2.24	1.01	Nagri Age	This study

TABLE 3 (continued).

Taxon	Locality	Elements (sample size)	Mean length (range) in mm	Mean width (range) in mm	Mean width/ length	Square root of width* Length	Mean ant./ mean Post.	Geological Formation	Reference
Sayimys sivalensis PUCT 7	Tappar, Kutch, India	m1/m2	2.05	Post: 1.7	0.83	1.87	_	Late Miocene (=Nagri)	Patnaik et al., 2022
Sayimys sivalensis (including *S. chinjiensis*)	Potwar Plateau, Pakistan	m1/m2 (L=21; W=27,22)	2.15 (1.78-2.50)	Ant: 1.85 (1.38-2.50) Post: 1.79 (1.42-2.18)	0.86	1.99	1.03	Kamlial, Chinji, and Nagri	Baskin,1996; Lopez Antonanzas & Sen, 2003
Sayimys sivalensis	Daud Khel, Potwar Plateau, Pakistan	m1 (L=33, W=33,33)	2.24 (2.00-2.60)	Ant: 1.90 (1.56-2.08) Post: 1.85 (1.60-2.08)	0.85	2.06	1.03	Chinji	Munthe, 1980
Sayimys sivalensis	Daud Khel, Potwar Plateau, Pakistan	m2 (L=28, W=28,28)	2.61 (2.32-2.80)	Ant: 2.48 (2.24-2.64) Post: 2.20 (1.80-2.68)	0.95	2.54	1.13	Chinji	Munthe, 1980
Sayimysbaskini (=Sayimys cf. *S. minor)*	YGSP721 Pakistan	m1/m2 (L=1; W=1,1)	1.65 (1.45-1.45)	Ant:1.45 Post: 1.45	0.88	1.55	1.00	Kamlial	Baskin, 1996
Sayimysbaskini (=Sayimys cf. *S. minor)*	YGSP747 Pakistan	m1/m2 (L=13; W=12,16)	2.02 (1.57-2.37)	Ant: 1.81 (1.50-2.07) Post: 1.72 (1.43-2.15)	0.90	1.91	1.05	Kamlial	Baskin, 1996
Sayimys cf. *S. intermedius*	Zinda Pir Dome and Potwar Plateau, Pakistan	m1/m2 (L=3; W=3,4)	1.95 (1.78-2.12)	Ant: 1.60 (1.50-1.75) Post: 1.61 (1.45-1.75)	0.82	1.77	0.99	Vihowa and Kamlial	Baskin, 1996

tephrochronology and mammalian bostratigraphy (Johnson et al., 1982, 1983, 1985; Barry and Flynn 1990; Flynn et al., 1995; Barry et al., 2002; Badgley et al., 2005, 2008; Pillans et al., 2005). This biochronological framework has become useful for correlating across Siwalik localities in South Asia (Flynn, 1982a, 1982b, 1986; Flynn et al., 2013; Wang et al., 2013 and references therein). The present locality exposed at Dunera was tentatively assessed as equivalent in geological age to the classic Chinji (Middle Miocene) or Nagri formations (Late Miocene) on the Potwar Plateau based on the few collected macromammal taxa (Vasishat et al., 1983). However, *Dorcatherium, Giraffokeryx,* and primitive bovids have relatively wide age ranges from the Middle to Late Miocene in the Siwaliks (Pilgrim, 1910; Colbert, 1935; Vasishat et al., 1983; Bhatti, 2005; Bhatti et al., 2007a, b, 2012; Khan et al., 2010), and a more precise age estimate for these sediments has been unavailable due to the lack of age diagnostic fossils. Based on paleomagnetic study of the broader Katilu Khad section, Sinha et al. (2005) suggested that the fossiliferous deposits at Dunera correlated to the long normal Chron 5n, which currently corresponds to Chron 5n.2n (Ogg, 2020), ranging between ~11.056 Ma at the base to ~9.984 Ma at the top. Sinha et al. (2005) suggested the locality of Dunera was close to the base of the normal chron, i.e., ~11 Ma.

Micromammals, especially rodents, contain numerous time-sensitive species, and have thus been heavily used in biostratigraphic analyses because they can help accurately estimate the geological age at a high resolution for localities where other geochronological dating methods are not available (Flynn et al., 1995). Thus, they provide an independent estimate that can be used in combination with other time-sensitive macromammal species as well as paleomagnetic data to accurately determine the geological age. Furthermore, they are very sensitive to climatic changes, which leads to change in community structure, allowing an analysis of the migration and reduction or extinction of certain groups (Patnaik and Sahni, 1996).

For the fossil rodents present at Dunera, the ctenodactylid rodent *Sayimys sivalensis* ranges from 15.2 to 9 Ma (Baskin, 1996; Flynn et al., 2013; Patnaik, 2013), the cricetine rodent *Democricetodon fejfari* ranges from 13.8 to 8.7 Ma (Lindsay, 2017), and the sciurid *Tamias urialis* ranges from 13.6 to 11.2 Ma (Munthe, 1980; Flynn, 2003; Flynn and Wessels, 2013; Bhandari et al., 2021; Flynn et

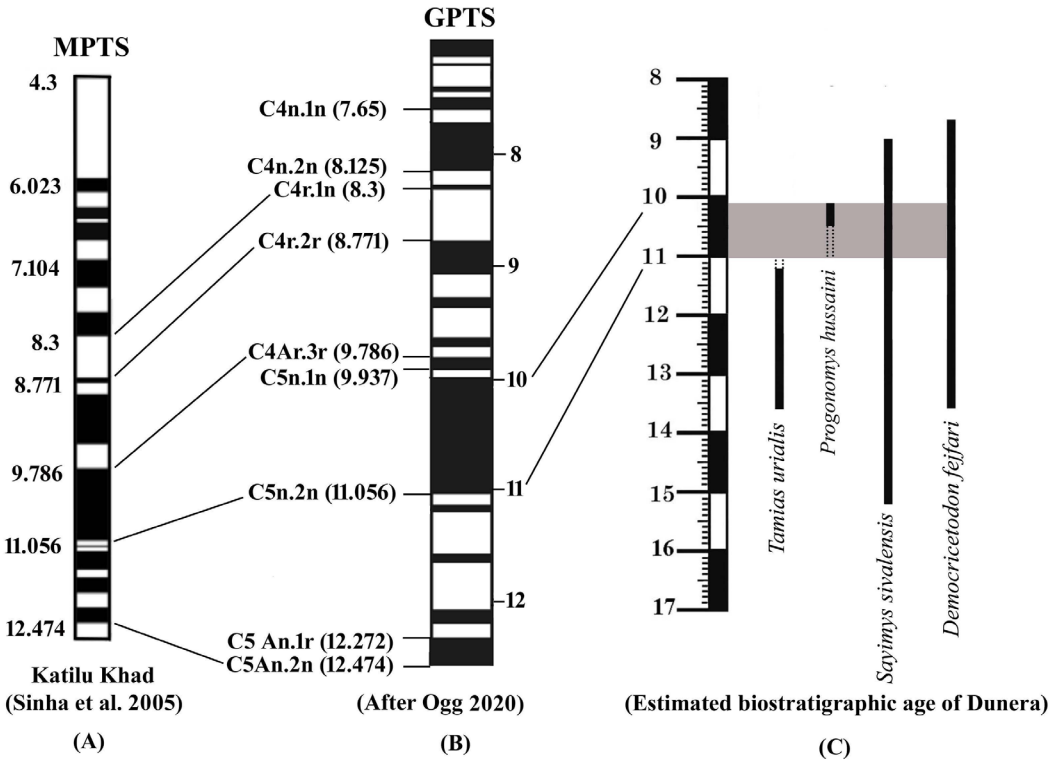

FIGURE 8. A) Magnetostratigraphy for the Katilu Khad section exposed nearby the Dunera town of Pathankot, Punjab (Sinha et al., 2005); B) Geomagnetic Polarity Time Scale (after Ogg, 2020); C) The proposed age of the present study locality (Dunera) against observed Potwar Siwalik rodent biochronology.

al., 2023) in the Siwaliks. The Dunera murine specimens possess mixed features that are most commonly associated with assemblages described as pre-*Progonomys* and *Progonomys hussaini*, thereby suggesting a likely age range at Dunera between ~11.6 and 10 Ma (Cheema et al., 2000; Flynn et al., 2020; Kimura et al., 2021). Based largely on the morphology preserved in the M1, here we favor a tentative assignment of the recovered murines to *P.* cf. *hussaini*, which has FAD ~10.5 Ma on the Potwar Plateau. However, we also highlight the gap in major Potwar micromammal sites between ~11.2 and 10.5 Ma, and so the first occurrence of *P. hussaini* could be earlier than the well-dated Potwar occurrence (Fynn et al., 2020; Kimura et al., 2021). Given the presence of the Dunera sciurid most similar to *T. urialis*, which has an LAD at ~11.2 Ma at Potwar sites, on biostratigraphic grounds, Dunera likely falls somewhere between the LAD of *T. urialis* and the LAD of *P. hussaini*, somewhere between ~11.2-10.1 Ma (Figure 8), and may fill in the aforementioned gap in the Siwaliks micromammal record between ~11.2-10.5 Ma. Indeed, paleomagnetic and stratigraphic data suggest that the Dunera assemblage falls near the base of a long normal paleomagnetic chron (see Sinha et al., 2005), with the most likely candidate being Chron 5n.2n ~11.056-9.984 Ma. If Dunera is at the base of this chron, it would be close to ~11.0 Ma, at the older end of the Potwar micromammal gap and equivalent to the lower part of the Nagri Formation in age. This age assessment requires a slight LAD range extension of ~150-200 Ka for *T. urialis* to ~11.0 Ma, and if the murine at Dunera is indeed *P. hussaini*, it would also represent a new FAD for this taxon (Figure 8). Given the current evidence, both of these temporal range extensions seem reasonable, and *P. hussaini* has previously been estimated to potentially range up to ~11.0 Ma on biostratigraphic ground at site JAL-101 in Pakistan (Cheema et al., 2000). Because cf. *Tamias urialis* at Dunera is only represented by two teeth, it is also possible that the species of *Tamias* found at Dunera is distinct from *T. urialis*. Additional specimens will be necessary to choose between these alternatives, but currently we consider it most parsimonious to tentatively assign the sciurid specimens to cf. *T. urialis* and

assume a slight LAD range extension for this taxon.

Due to its proximity, it is likely that Dunera was part of the same biogeographical province as the Potwar Plateau during the Middle to early Late Miocene. Thus, the potential age range extensions of *P.* cf. *hussaini* and cf. *T. urialis* almost certainly reflect increased sampling of an underrepresented time period in the greater Siwaliks region rather than documenting these species spanning a drastically different time period in a different biogeographic region. Further work at Dunera will be important in helping to elucidate this undersampled time period in Siwalik mammalian evolutionary history.

ACKNOWLEDGEMENTS

R.K.S., A.P.S., and N.P.S. thank the Director, Wadia Institute of Himalayan Geology, Dehradun for the research facilities (contributin no. WIHG/0284). N.P.S. is supported by SERB DST (SRG/2023/000041). This reseach was also supported, in part, by U.S. National Science Foundation BCS Award 1945736 to C.C.G. and BCS Award 1945618 to B.A.P. We thank T. Skorka, T. Jashashvili, and the University of Southern California's Molecular Imaging Center (MIC) for assistance with uCT scanning. We thank L. Flynn for helpful advice and the three anonymous reviewers for their constructive feedback and comments to improve the manuscript. We would also like to thank the handling editor M. Stewart for his editorial work.

REFERENCES

Azzaroli, A. and Napoleone, G. 1982. Magnetostratigraphic investigation of the Upper Siwaliks near Pinjaur, India. Rivista Italiana Paleontologia e Stratigrafia, 87(4):739–762.

Badgley, C., Barry, J.C., Morgan, M.E., Nelson, S.V., Behrensmeyer, A.K., Cerling, T.E., and Pilbeam, D. 2008. Ecological changes in Miocene mammalian record show impact of prolonged climatic forcing. Proceedings of the National Academy of Sciences, 105(34):12145–12149. https://doi.org/10.1073/pnas.0805592105

Badgley, C., Nelson, S., Barry, J.C., Behrensmeyer, A.K., and Cerling T.E. 2005. Testing models of faunal turnover with Neogene mammals from Pakistan, p. 29–46. In Lieberman, D.E., Smith, R.H., and Kelley, J. (eds.), Interpreting the Past: Essays on Human, Primate, and Mammal Evolution. Boston, Brill.

Barry, J.C. and Flynn, L.J. 1990. Key Biostratigraphic Events in the Siwalik Sequence, p. 557–571. In Lindsay, E.H., Fahlbusch, V., and Mein, P. (eds.), European Neogene Mammal Chronology, vol. 180. NATO ASI Series, Springer, Boston, MA.

Barry, J.C., Behrensmeyer, A.K., Badgley, C.E., Flynn, L.J., Peltonen, H., Cheema, I.U., Pilbeam, D., Lindsay, E.H., Raza, S.M., Rajpar, A.R., and Morgan, M.E. 2013. The Neogene Siwaliks of the Potwar Plateau, Pakistan, p. 373–399. In Fortelius, M., Wang, X., and Flynn, L.J. (eds.), Fossil Mammals of Asia: Neogene Biostratigraphy and Chronology. Columbia University Press, New York. https://doi.org/10.7312/columbia/9780231150125.003.0015

Barry, J.C., Johnson, N.M., Raza, S.M., and Jacobs, L.L. 1985. Neogene mammalian faunal change in southern Asia: Correlations with climate, tectonic and eustatic events. Geology, 13(9):637–640. https://doi.org/10.1130/0091-7613(1985)13<637:NMFCIS>2.0.CO;2

Barry, J.C., Lindsay, E.H., and Jacobs, L.A. 1982. A biostratigraphic zonation of the Middle and Upper Siwaliks of the Potwar Plateau of northern Pakistan. Palaeogeography, Palaeoclimatology, Palaeoecology, 37(1):95–130. https://doi.org/10.1016/0031-0182(82)90059-1

Barry, J.C., Morgan, M.E., Flynn, L.J., Pilbeam, D., Behrensmeyer, A.K., Raza, S.M., Khan, I.A., Badgley, C., Hicks, J., and Kelley, J. 2002. Faunal and environmental change in the Late Miocene Siwaliks of northern Pakistan. Paleobiology Memoirs, 3:1–71. https://doi.org/10.1666/0094-8373(2002)28[1:FAECIT]2.0.CO;2

Baskin, J.A. 1996. Systematic revision of Ctenodactylidae (Mammalia, Rodentia) from the Miocene of Pakistan. Palaeovertebrata, 25:1–49.

Basu, P.K. 2004. Siwalik mammals of the Jammu Sub-Himalayan, India: an appraisal of their diversity and habitat. Quaternary International, 117(1):105–118. https://doi.org/10.1016/S1040-6182(03)00120-4

Bhandari, A., Bajpai, S., Flynn, L.J., Tiwari, B.N., and Mandal, N. 2021. First Miocene rodents from Kutch, western India. Historical Biology, 33(12):3471–3479. https://doi.org/10.1080/08912963.2020.1870970

Bhatti, Z.H. 2005.Taxonomy, evolutionary history and biogeography of the Siwalik giraffids. Unpublished PhD thesis, University of the Punjab, Pakistan.

Bhatti, Z.H., Khan, M.A., Akhtar, M., Khan, M.A., Ghaffar, A., Iqbal, M., and Ikram, T. 2012. *Giraffokeryx* (Artiodactyla: Mammalia) remains from the lower Siwaliks of Pakistan. Pakistan Journal of Zoology, 44(6):1623–1631.

Bhatti, Z.H., Qureshi, M.A., Khan, M.A., Akhtar, M., Ghaffar, A., and Ejaz, M. 2007a. Individual variations in some premolars of species *Giraffokeryx punjabiensis* (Mammalia, Giraffidae) from Lower Siwalik (Chinji Formation) of Pakistan. Contribution to Geology of Pakistan (Proceedings of the 5th Pakistan Geological Congress), National Geological Society, Pakistan, 5:261–272.

Bhatti, Z.H., Qureshi, M.A., Khan, M.A., Akhtar, M., Ghaffar, A., and Ejaz, M. 2007b. Fossil remains of the species *Giraffa priscilla* (Mammalia, Giraffidae) from the Lower Siwaliks (Chinji Formation) of Pakistan. Contribution to Geology of Pakistan (Proceedings of the 5th Pakistan Geological Congress), National Geological Society, Pakistan, 5:273–284.

Bosma, A.A., de Bruijn, H., and Wessels, W. 2013. Late Miocene Sciuridae (Mammalia, Rodentia) from Anatolia, Turkey. Journal of Vertebrate Paleontology, 33(4):924–942. https://doi.org/10.1080/02724634.2013.755990

Bosma, A.A., de Bruijn, H., and Wessels, W. 2018. Early and middle Miocene Sciuridae (Mammalia, Rodentia) from Anatolia, Turkey. Journal of Vertebrate Paleontology, 38(6):e1537281. https://doi.org/10.1080/02724634.2018.1537281

Brown, B., Gregory, W.K., and Hellman, M. 1924. On three incomplete anthropoid jaws from the Siwaliks, India. American Museum Novitates, 130:1–9.

Cande, S.C. and Kent, D.V. 1995. Revised calibration of the geomagnetic polarity timescale for the Late Cretaceous and Cenozoic. Journal of Geophysical Research, 100(B4):6093–6095. https://doi.org/10.1029/94JB03098

Cheema, I.U., Raza, S.M., Flynn, L.J., Rajpar, A.R., and Tomida, Y. 2000. Miocene small mammals from Jalalpur, Pakistan, and their Biochronologic Implications: Bulletin of the National Science Museum, Tokyo, ser. C, 26 (1, 2):57–77.

Cheema, I.U., Sen, S., Flynn, L.J. 1983. Early Vallesian small mammals from the Siwaliks of northern Pakistan. Bulletin du Muséum National d'Histoire Naturelle, Paris, 4e, Ser. 5, Section C, no. 3:267–280.

Chirouze, F., Dupont-Nivet, G., Huyghe, P., van der Beek, P., Chakraborti, T., Bernet, M., and Erens, V. 2012. Magnetostratigraphy of the Neogene Siwalik Group in the far eastern Himalaya: Kameng section, Arunachal Pradesh, India. Journal of Asian Earth Sciences, 44:117–135. https://doi.org/10.1016/j.jseaes.2011.05.016

Chopra, S.R.K. 1983. Significance of the recent hominoid discoveries from the Siwalik hills of India, p. 539–557. In Ciochon, R.L. and Corruccini, R.S. (eds.), New Interpretations of Ape and Human Ancestry. Plenum, New York.

Colbert, E.H. 1935. Siwalik mammals in the American Museum of Natural History. Transactions of the American Philosophical Society, 26:1–401. https://doi.org/10.2307/1005467

de Bruijn, H., Hussain, S.T., and Leinder, J.J.M. 1981. Fossil rodents from the Murree Formation near Banda Daud Shah, Kohat, Pakistan. Proceedings of the Koninklijke Nederlandse Akademie van Wetenschappen, Series B, 84(1):71–99.

Fahlbusch, V. 1964. Die Cricetiden (Mammalia) der Oberen Süßwasser-Molasse Bayerns. Abhandlungen der Bayerisch Akademie der Wissenschaften, Neue Folge, 118:1–136.

Fahlbusch, V. 1969. Pliozäne und Pleistozäne Cricetinae (Rodentia, Mammalia) aus Polen. Acta Zoologica Cracoviensia, 14:99–138.

Fischer de Waldheim, G. 1817. Adversaria Zoologica. Mémoires de la Société Impériale des Naturalistes de Moscou, 5:357–471.

Flynn, L.J. 1982a. A revision of fossil Rhizomyid rodents from Northern India and their correlation to a Rhizomyid biochronology of Pakistan. Geobios, 15(4):583–588. https://doi.org/10.1016/S0016-6995(82)80074-0

Flynn, L.J. 1982b. Systematic revision of Siwalik Rhizomyidae (Rodentia). Geobios, 15(3):327–389. https://doi.org/10.1016/S0016-6995(82)80084-3

Flynn, L.J. 1986. Species longevity, stasis, and stair steps in rhizomyid rodents, p. 273–285. In Flanagan, K.M. and Lillegraven, J.A. (eds.), Vertebrates, Phylogeny and Philosophy. Contributions to Geology, University of Wyoming Special Paper, 3.

Flynn, L.J. 2003. Small mammal indicators of forest paleoenvironment in the Siwalik deposits of the Potwar Plateau, Pakistan, p. 183–196. In Reumer, J.W.F. and Wessels, W. (eds.), Distribution and migration of Tertiary mammals in Eurasia. A volume in honour of Hans de Bruin, Deinsea, 10.

Flynn, L.J. and Wessels, W. 2013. Paleobiogeography and South Asian small mammals, p. 445–460. In Wang, X., Flynn, L.J., and Fortelius, M. (eds.), Fossil Mammals of Asia. Columbia University Press.

Flynn, L.J., Barry, J.C., Morgan, M.E., Pilbeam, D., Jacobs, L.L., and Lindsay, E.H. 1995. Neogene Siwalik mammalian lineages: Species longevities, rates of change, and modes of speciation. Palaeogeography, Palaeoclimatology, Palaeoecology, 115:249–264. https://doi.org/10.1016/0031-0182(94)00114-N

Flynn, L.J., Kimura, Y., and Jacobs, L.J. 2020. The murine cradle, p. 347–362. In Prasad, G.V.R. and Patnaik, R. (eds.), Biological consequences of plate tectonics. Vertebrate Paleobiology and Paleoanthropology Series.

Flynn, L.J., Lindsay, E.H., Pilbeam, D., Raza, S.M., Morgan, M.E., Barry, J.C., Badgley, C.E., Behrensmeyer, A.K., Cheema, I.U., Rajpar, A.R., and Opdyke, N.D. 2013. The Siwaliks and Neogene evolutionary biology in South Asia, p. 353–372. In Wang, X., Flynn, L.J., and Fortelius, M. (eds.), Fossil mammals of Asia: Neogene biostratigraphy and chronology. Columbia University Press, New York.

Flynn, L.J., Morgan, M.E., Barry, J.C., Raza, S.M., Cheema, I.U., and Pilbeam, D. 2023. Siwalik Rodent Assemblages for NOW: Biostratigraphic Resolution in the Neogene of South Asia, p. 43–58. In Casanovas-Vilar, I., van den Hoek Ostende, L.W., Janis, C.M., and Saarinen, J. (eds.), Evolution of Cenozoic Land Mammal Faunas and Ecosystems. Vertebrate Paleobiology and Paleoanthropology. Springer, Cham. https://doi.org/10.1007/978-3-031-17491-9_4

Gaur, R. and Chopra, S.R.K. 1983. Palaeoecology of the middle Miocene Sivalik sediments of a part of Jammu and Kashmir State, India. Palaeogeography, Palaeoclimatology, Palaeoecology, 43(3-4):313–327. https://doi.org/10.1016/0031-0182(83)90016-0

Gilbert, C.C., Ortiz, A., Pugh, K.D., Campisano, C.J., Patel, B.A., Singh, N.P., Fleagle, J.G., and Patnaik, R. 2020. New Middle Miocene ape (Primates: Hylobatidae) from Ramnagar, India fills major gaps in the hominoid fossil record. Proceedings of the Royal Society B, Biological Sciences, 287:20201655. https://doi.org/10.1098/rspb.2020.1655

Gilbert, C.C., Patel, B.A., Singh, N.P., Campisano, C.J., Fleagle, J.G., Rust, K.L., and Patnaik, R. 2017. New sivaladapid primate from Lower Siwalik deposits surrounding Ramnagar, Jammu and Kashmir state, India. Journal of Human Evolution, 102:21–41. https://doi.org/10.1016/j.jhevol.2016.10.001

Gilbert, C.C., Sehgal, R.K., Pugh, K.D., Campisano, C.J., May, E., Patel, B.A., Singh, N.P., and Patnaik, R. 2019. A new *Sivapithecus* specimen from Ramnagar (Jammu and Kashmir), India and a taxonomic revision of Ramnagar hominoids. Journal of Human Evolution, 135:102665. https://doi.org/10.1016/j.jhevol.2019.102665

Gregory, W.K., Hellman, M., and Lewis, G.E. 1938. Fossil Anthropoids of the Yale-Cambridge India expedition of 1935. Carnegie Institute of Washington.

Hinton, M.A.C. 1933. Diagnoses of new genera and species of rodents from Indian Tertiary deposits. Annals and Magazine of Natural History, 12(72):620–622. https://doi.org/10.1080/00222933308673728

Illiger, J.K.W. 1811. Prodromus systematis mammalium et avium. C. Salfeld, Berlin. https://doi.org/10.5962/bhl.title.106965

Jacobs, L.L. 1978. Fossil rodents (Rhizomyidae and Muridae) from Neogene Siwalik deposits, Pakistan. Museum of Northern Arizona Press Bulletin Series, 52:1–103.

Jacobs, L.L., Flynn, L.J., and Downs, W.R. 1989. Neogene rodents of Southern Asia, p. 157–177. In Black, C.C. and Dawson, M.R. (eds.), Papers on Fossil Rodents in Honour of Albert Elmer Wood. Natural History Museum of Los Angeles County, Special Publication, 33.

Johnson, G.D., Opdyke, N.D., Tandon, S.K., and Nanda, A.C. 1983. The magnetic polarity stratigraphy of the Siwalik Group at Haritalyangar (India) and a new last appearance datum for *Ramapithecus* and *Sivapithecus* in Asia. Palaeogeography, Palaeoclimatology, Palaeoecology, 44:223–249. https://doi.org/10.1016/0031-0182(83)90105-0

Johnson, N.M. and McGee, V.E. 1983. Magnetic polarity stratigraphy: Stochastic properties of data, sampling problems and the evaluation of interpretations. Journal of Geophysical Research, 88(B2):1213–1221. https://doi.org/10.1029/JB088iB02p01213

Johnson, N.M., Opdyke, N.D., Johnson, G.D., Lindsay, E.H., and Tahirkheli, R.A.K. 1982. Magnetic polarity stratigraphy and ages of Siwalik Group rocks of the Potwar Plateau, Pakistan. Palaeogeography, Palaeoclimatology, Palaeoecology, 37(1):17–42. https://doi.org/10.1016/0031-0182(82)90056-6

Johnson, N.M., Stix, J., Tauxe, L., Cerveny, P.F., Tahirkheli, R.A.K. 1985. Paleomagnetic chronology, fluvial processes, and tectonic implications of the Siwalik deposits near Chinji Village, Pakistan. The Journal of Geology, 93(1):27–40. https://doi.org/10.1086/628917

Khan, M.A., Butt, S.S., Khan, A.M., and Akhtar, M. 2010. A new collection of *Giraffokeryx punjabiensis* (Giraffidae, Ruminantia, Artiodactyla) from the Lehri Outcrops, Jhelum, Northern Pakistan. Pakistan Journal of Science, 62(2):120–123.

Kimura, Y., Jacobs, L.L., and Flynn, L.J. 2013. Lineage-specific responses of tooth shape in murine rodents (Murinae, Rodentia) to Late Miocene dietary change in the Siwaliks of Pakistan. PLoS ONE, 8:e76070. https://doi.org/10.1371/journal.pone.0076070

Kimura, Y., Flynn, L.J., and Jacobs, L.L. 2017. Early Late Miocene murine rodents from the upper part of the Nagri Formation, Siwalik Group, Pakistan, with a new fossil calibration point for the tribe Apodemurini (*Apodemus/Tokudaia*). Fossil Imprint, 73(1-2):197–212. https://doi.org/10.2478/if-2017-0011

Kimura, Y., Flynn, L.J., and Jacobs, L.L. 2021. Tempo and mode: evidence on a protracted split from a dense fossil record. Frontiers in Ecology and Evolution, 9:642814. https://doi.org/10.3389/fevo.2021.642814

Kotlia, B.S., Phartiyal, B., Kosaka, T., and Bohra, A. 2008. Magnetostratigraphy and lithology of Miocene-Pliocene Siwalik deposits between Tanakpur and Sukhidang, southeastern Uttarakhand Himalaya, India. Himalyan Geology, 29(2):127–136.

Kumaravel, V., Sangode, S.J., Kumar, K., and Siva Siddaiah, N. 2005. Magnetic polarity stratigraphy of Plio-Pleistocene Pinjor formation (type locality), Siwalik Group, NW Himalaya, India. Current Science, 88(9):1453–1461.

Lindsay, E.H. 2017. *Democricetodon fejfari* sp. nov. and replacement of Cricetidae by Muridae in Siwalik deposits of Pakistan. Fossil Imprint, 73(3-4):445–453. https://doi.org/10.2478/if-2017-0022

Lindsay, E.H. and Flynn, L.J. 2016. Late Oligocene and Early Miocene Muroidea of the Zinda Pir Dome. Historical Biology, 28(1-2):215–236. https://doi.org/10.1080/08912963.2015.1027888

López-Antoñanzas, R. and Sen, S. 2003. Systematic revision of Mio-Pliocene Ctenodactylidae (Mammalia, Rodentia) from the Indian subcontinent. Eclogae Geologicae Helvetiae, 96:521–529. http://doi.org/10.5169/seals-169037

Maridet, O., Wu, W.-Y., Ye, J., Bi, S.-D., Ni, X.-J., and Meng, J. 2011. Earliest occurrence of *Democricetodon* in China, in the Early Miocene of the Junggar Basin (Xinjiang) and comaparison with the genus *Spanocricetodon*. Vertebrata Palasiatica, 49(4):393–405.

Munthe, J. 1980. Rodents of the Miocene Daud Khel local fauna, Mianwali District, Pakistan. Part 1. Sciuridae, Gliridae, Ctenodactylidae, and Rhyzomyidae. Contributions in Biology and Geology, Milwaukee Public Museum, 34:1–36.

Nanda, A.C. and Sehgal, R.K. 1993. Siwalik mammalian faunas from Ramnagar (J. & K.) and Nurpur (H.P.) and lower limit of hipparion. Journal of the Geological Society of India, 42(2):115–134.

Nowak, R.M. 1999. Walker's Mammals of the World, Sixth Edition, Volume 2. Johns Hopkins University Press, Baltimore.

Ogg, J.G. 2020. Geomagnetic polarity time scale, p. 159–192. In Gradstein, F.M., Ogg, J.G., Schmitz, M.D., and Ogg, G.M. (eds.), Geologic time scale 2020, 1st edition. Elsevier Publication.
https://doi.org/10.1016/B978-0-12-824360-2.00005-X

Osborn, H.F. 1910. The age of mammals in Europe, Asia and North America. New York, the Macmillan Company.
https://doi.org/10.5962/bhl.title.39523

Parmar, V. 2013. Fossil molluscs from the Middle Miocene Lower Siwalik deposits of Jammu, India. International Research Journal of Earth Sciences, 1(1):16–23.

Parmar, V. and Jigmet, T. 2014. First Fossil Discoglossinae (Anura) from the Siwaliks of the Indian Subcontinent. International Research Journal of Earth Sciences, 2(8):1–6.

Parmar, V. and Prasad, G.V.R. 2006. Middle Miocene rhizomyid rodent (Mammalia) from the Lower Siwalik Subgroup of Ramnagar, Udhampur District, Jammu and Kashmir, India. Neues Jahrbuch für Geologie and Paläontologie-Monatshefte Jg., 6:371–384.
https://doi.org/10.1127/njgpm/2006/2006/371

Parmar, V. and Prasad, G.V.R. 2012. Fossil fish fauna from the Lower Siwalik beds of Jammu. Journal of the Palaeontological Society of India, 57(1):43–52.

Parmar, V., Prasad, G.V.R., Kumar, J., Malik, M.A., and Norboo, R. 2015. Cricetid rodents from the Lower Siwalik Subgroup of Jammu, India: biochronological significance. Palaeoworld, 24(3):324–335.
https://doi.org/10.1016/j.palwor.2014.12.002

Parmar, V., Prasad, G.V.R., and Norboo, R. 2018. Middle Miocene small mammals from the Siwalik Group of Northwestern India. Journal of Asian Earth Science, 162:84–92.
https://doi.org/10.1016/j.jseaes.2017.11.023

Parmar, V., Norboo, R., Magotra, R., and Kshetrimayum, D.S. 2022. Cricetid rodents from the Middle Miocene Siwalik exposure of Kalaunta (Jammu), NW Himalaya, India. Arabian Journal of Geosciences, 15:1569.
https://doi.org/10.1007/s12517-022-10849-1

Parmar, V., Norboo, R., and Magotra, R. 2023. First record of Erinaceidae and Talpidae from the Miocene Siwalik deposits of India. Historical Biology, 35(2):276–283.
https://doi.org/10.1080/08912963.2022.2034806

Patnaik, R. 2013. Indian Neogene Siwalik mammalian biostratigraphy: an overview, p. 423–444. In Wang, X., Flynn, L.J., and Fortelius, M. (eds.), Fossil mammals of Asia: Neogene biostratigraphy and chronology. Columbia University Press, New York.

Patnaik, R. and Sahni, A. 1996. Siwalik rodent biostratigraphy: implications for intra-subcontinental correlation, p. 557–571. In Pandey, J., Azmi, R.J., Bhandari, A., and Dave, A. (eds.), Contributions to XVI Indian Colloquium on Micropalaeontology and Stratigraphy, Dehradun.

Patnaik, R. Singh, N.P., Sharma, K.M., Singh, N.A., Choudhary, D., Y. Singh, Y.P., Kumar, R., Wazir, W.A., and Sahni, A. 2022. New rodents shed light on the age and ecology of late Miocene ape locality of Tapar (Gujarat, India). Journal of Systematic Palaeontology, 20(1):2084701.
https://doi.org/10.1080/14772019.2022.2084701

Pilgrim, G.E., 1910. Preliminary note on a revised classification of the Tertiary freshwater deposits of India. Records of the Geological Survey of India, 40:185–205.

Pilgrim, G. E. 1927. A *Sivapithecus* palate and other primate fossils from India. Paleontologica Indica, 14:1–24.

Pillans, B., Williams, M., Cameron, C., Patnaik, R., Hogarth, J., Sahni, A., Sharma, J.C., Williams, F., and Bernor, R.L., 2005. Revised correlation of the Haritalyangar magnetostratigraphy, Indian Siwaliks: Implications for the age of the Miocene hominids *Indopithecus* and *Sivapithecus*, with a note on a new hominid tooth. Journal of Human Evolution, 48(5):507–515.
https://doi.org/10.1016/j.jhevol.2004.12.003

Ranga Rao, A., Agarwal, R.P., Sharma, U.N., Bhalla, M.S., and Nanda, A.C. 1988. Magnetic polarity stratigraphy and vertebrate palaeontology of the Upper Siwalic subgroup of Jammu Hills, India. Journal of Geological Society of India, 31(4):361–385.

Ranga Rao, A., Nanda, A.C., Sharma, U.N., and Bhalla, M.S. 1995. Magnetic polarity stratigraphy of the Pinjor Formation (Upper Siwalik) near Pinjor, Haryana. Current Science, 68(12):1231–1236.

Raiverman, V. 2002. Foreland Sedimentation in Himalayan Tectonic Regime: A relook at the orogenic process. Bisen Singh Mahendra Pal Singh Publication, Dehradun.

Rangaraj, S. 1978. Stratigraphy and Sedimentology of Siwalik Molasse in a part of Punjab Sub-Himalaya. Unpublished PhD thesis, University of Delhi.

Sangode, S.J., Kumar, R., and Ghosh, S.K. 1996. Magnetic polarity stratigraphy of the Siwalik sequence of Haripur area (HP), NW Himalaya. Geological Society of India, 47(6):683–704.

Schaub, S. 1938. Tertiäre und Quartäre Murinae. Abhandlungen des Schweizerischen paläontologischen Gesellschaft, 61:1–38.

Sehgal, R.K. 1998. Lower Siwalik carnivores from Ramnagar (J. & K.). Himalayan Geology, 19 (1):109–118.

Sehgal, R.K. and Patnaik, R. 2012. New muroid rodent and *Sivapithecus* dental remains from the Lower Siwalik deposits of Ramnagar, Jammu and Kashmir: age implication. Quaternary International, 269:69–73. https://doi.org/10.1016/j.quaint.2011.01.043

Sehgal, R.K., Singh, A.P., Gilbert, C.C., Patel, B.A., Campisano, C.J., Selig, K.R., Patnaik, R., and Singh, N.P. 2022. A new genus of treeshrew and other micromammals from the middle Miocene hominoid locality of Ramnagar, Udhampur District, Jammu & Kashmir State, India. Journal of Palaeontology, 96(6):1318–1335. https://doi.org/10.1017/jpa.2022.41

Singh, N.P., Gilbert, C.C., Patel, B.A., and Patnaik, R. 2018. The taphonomy and palaeoecology of the Middle Miocene hominoid locality of Ramnagar (Jammu and Kashmir, India): Journal of Asian Earth Sciences, 162:69–83. https://doi.org/10.1016/j.jseaes.2018.02.020

Sinha, S., Islam, R, Ghosh, S.K., Kumar, R., and Sangode, S.J. 2007. Geochemistry of Neogene Siwalik mudstones along Punjab re-entrant, India: Implications for source-area weathering, provenance and tectonic setting. Current Science, 92(8):1103–1113.

Sinha, S., Sangode, S.J., Kumar, R., Ghosh, S.K. 2005. Accumulation history and tectonic significance of the Neogene continental deposits in the west central sector of the Himalayan foreland basin. Himalayan Geology, 26(2):387–408.

Tandon, S.K. and Rangaraj, S. 1979. Sedimentary tectonics of the Siwalik Sequence, south east of Ravi structural Re-entrant, p. 273–282. In Saklani, P.S. (ed.), Structural Geology of Himalaya. Today and Tomorrow, Delhi.

Tandon, S.K., Kumar, R., Koyama, M., and Niitsuma, N. 1984. Magnetic polarity stratigraphy of the Upper Siwalik Subgroup, east of Chandigarh, Punjab sub-Himalaya, India. Journal of Geological Society of India, 25(1):45–55.

Thomas, H. and Verma, S.N. 1979. Decouverte d'un Primate Adapiforme (Sivaladapinae sub. fam. nov.) dans le Miocene moyen des Siwaliks de la region de Ramnagar (Jammu et Cachemire, Inde). Comptes Rendus Hebdomadaires des Seances de l'Academie des Sciences serie D: Sciences Naturelles, 289(12):833–836.

Vasishat, R.N., Gaur, R., and Chopra, S.R.K. 1978. Geology, fauna and palaeoenvironments of Lower Sivalik deposits around Ramnagar, India. Nature, 275:736–737. https://doi.org/10.1038/275736a0

Vasishat, R.N., Gaur, R., and Chopra, S.R.K. 1985. First record of *Dorcatherium nagrii* (tragulidae, Mammalia) from Lower Siwaliks of Ramnagar area (J & K), India. Journal of the Palaeontological Society of India, 30:59–62.

Vasishat, R.N., Gaur, R., Suneja I.J., and Chopra, S.R.K. 1983. On a new Neogene fossil locality near Dunera, Gurdaspur District, Punjab, India. Current Science, 52(18):875–877.

Vasishat, R.N., Kaul, S., and Chopra, S.R.K. 1979. Additional fossil suid material from the Lower Siwalik of Ramnagar, Jammu and Kashmir State, India. Geological Survey of India, Miscellaneous Publication, 45:219–225.

Verma, B.C., Mishra, V.P., and Gupta, S.S. 2002. Pictorial catalogue of Siwalik vertebrate fossils from northwest Himalaya. Geological Survey of India, Catalogue series, 5:1–377.

Wang, X., Flynn, L.J., and Fortelius, M. 2013. Fossil Mammals of Asia: Neogene Biostratigraphy and Chronology. Columbia University Press, New York.
Wessels, W. and Reumer, B.M. 2009. Democricetodon and Megacricetodon (Mammalia, Cricetidae) from the Miocene of Sandelzhausen, Southern Germany. Paläontologische Zeitschrift, 83:187–205. https://doi.org/10.1007/s12542-009-0006-8
Wessels, W., de Bruijn, H., Hussain, S.T., and Leinders, J. 1982. Fossil rodents from the Chinji Formation, Banda Daud Shah, Kohat, Pakistan. Proceedings of the Koninklijke Nederlandse Akademie Van Wetenschappen Series B, 85(3):337–364.
Wilson, D.E. and Reeder, D.M. 2005. Mammal Species of the World: A Taxonomic and Geographic Reference, Third Edition, Volume 2. Johns Hopkins University Press, Baltimore.
Wood, A.E. 1937. Fossil rodents from the Siwalik beds of India. American Journal of Science, 34:64–76. https://doi.org/10.2475/ajs.s5-34.199.64
Yokoyama, T. 1981. Palaeomagnetic study of Tatrot and Pinjor Formation, Upper Siwalik, East of Chandigarh, Northwest India, p. 217–220. In Sastry, M.V.A., Kurien, T.K., Dutta, A.K., and Biswas, S. (eds.), Field conference Neogene/Quaternary Boundary, India, 1979. Proceedings of the Geological Survey of India, Calcutta.
Zhu-Ding, Q. 2010. Cricetid rodents from the Early Miocene Xiacaowan Formation, Sihong, Jiangsu. Vertebrata PalAsiatica, 48(1):27–47.
Zittel, K.A. 1893. Handbuch der Palaeontologie. 1 Abt. Palaeozoologie, Bd. IV. Mammalia. R. Oldenbourg, Munich and Leipzig.

APPENDIX

Comparative dental measurements (mm) of Dunera murine and previously described Siwalik fossil murines. (Available for download at https://palaeo-electronica.org/content/2023/4011-rodents-from-dunera-india.)